NASA Technical Memorandum 85773

Aerothermal Performance and Damage Tolerance of a René 41 Metallic Standoff Thermal Protection System at Mach 6.7

Don E. Avery
Langley Research Center
Hampton, Virginia

National Aeronautics
and Space Administration

**Scientific and Technical
Information Branch**

1984

SUMMARY

A flight-weight, metallic thermal protection system (TPS) model applicable to Earth-entry and hypersonic-cruise vehicles was subjected to multiple cycles of both radiant and aerothermal heating in order to evaluate its aerothermal performance, structural integrity, and damage tolerance. The TPS is a mass-optimized (1.491 lb/ft^2), shingled, radiative structure constructed of René 41, a nickel-base alloy. The TPS was designed for a maximum operating temperature of 2060°R and features a shingled, corrugation-stiffened corrugated-skin heat shield with insulation and beaded support ribs. The insulation package for the René 41 TPS consists of 1.38 in. of Micro-Quartz[1] fibers and 0.60 in. of HITCO TG 15000[2] fibers which are compressed by 10 percent.

The TPS model was evaluated in the Langley 8-Foot High-Temperature Tunnel. The model was subjected to 10 radiant-heating tests and to 3 radiant preheat/aerothermal-heating tests (representative of a Space Shuttle entry temperature history, or trajectory). The aerothermal tests were conducted at a nominal free-stream Mach number of 6.7, a stagnation temperature of approximately 3250°R, and a Reynolds number of approximately 1.4×10^6 per foot. The model outer surface was maintained at the approximate maximum operating temperature of 2060°R for a total of 63.7 minutes and was exposed to a hypersonic stream for a total of 53 sec.

Under radiant heating conditions with a maximum surface temperature of 2050°R, the TPS performed to design specifications and limited the primary structure away from the support ribs to temperatures below 780°R. During the first attempt at aerothermal exposure, a failure in the panel-holder test fixture severely damaged the model. However, two radiant preheat/aerothermal tests were made with the damaged model to determine its damage tolerance. During these tests, the damaged area did not enlarge; however, the rapidly increasing structural temperature measured during these tests indicates that had the damaged area been exposed to aerodynamic heating for the entire trajectory, the aluminum would have burned through. The severity of a burn-through would depend on its location on a vehicle. When the model was damaged in the wind-tunnel test, the fibrous insulation in the damaged area was immediately sucked out. The damage tolerance of the TPS could be improved by packaging the insulation so that it would remain at least partially intact when penetration damage to the heat shield occurs, thereby lowering the primary-structure temperature and preventing or delaying burn-through.

INTRODUCTION

Future hypersonic-cruise and Earth-entry vehicles will require lightweight, durable thermal protection systems (TPS's). Researchers at the Langley Research Center have been conducting a broad-based program to advance the state of the art for metallic TPS technology because of the inherent durability of metallic systems. Past investigations (refs. 1 to 4) have demonstrated the feasibility of shingled, radiative metallic TPS's; however, early metallic systems were heavier (ref. 4 and fig. 6

---

[1]Micro-Quartz: Registered trademark of Johns-Manville Corp.
[2]HITCO TG 15000: Registered trademark of HITCO.

of ref. 5) than the fused-silica reusable surface insulation (RSI) currently being used on the Space Shuttle orbiter (ref. 6). Therefore, recent studies have focused on mass optimization for the overall system.

A René 41 (nickel-base alloy) TPS was designed and fabricated under the Langley program. A model representative of the René 41 TPS features a corrugation-stiffened corrugated-skin heat shield, beaded support ribs, and insulation. The René 41 TPS was designed for operation at temperatures up to 2060°R. The area where a René 41 TPS could be used on the Space Shuttle orbiter is shown in figure 1.

The aerothermal performance, structural integrity, and damage tolerance of a 24- by 36-in. René 41 TPS model were evaluated in the Langley 8-Foot High-Temperature Tunnel, and this evaluation is the subject of this report. The model was subjected to 10 radiant-heating tests and to 3 radiant preheat/aerothermal-heating tests (representative of a Space Shuttle entry temperature history, or trajectory). The aerothermal-heating tests were conducted at a nominal free-stream Mach number of 6.7, a nominal stagnation temperature of about 3250°R, and a Reynolds number of approximately 1.4×10^6 per foot.

SYMBOLS

The measurements and calculations were made in U.S. Customary Units.

M_ℓ	local Mach number
M_∞	free-stream Mach number
q_∞	dynamic pressure, psia
R	unit Reynolds number, per foot
T	temperature, °R
$T_{t,c}$	total temperature in combustor, °R
t	time, sec
α	angle of attack, deg

Abbreviations:

av	average
max	maximum
rad	radius
ref	reference
reqd	required
typ	typical
TC	thermocouple

APPARATUS

Thermal Protection System

The thermal protection system (TPS) model was designed and fabricated by Grumman Aerospace Corporation under contract to the NASA Langley Research Center. The design is based on proven baseline concepts with mass optimization as the major concern (ref. 7).

Design criteria.- The René 41 TPS is designed to protect the primary structure from high surface temperatures typical of those expected during 100 entry cycles of the Space Shuttle orbiter. The surface temperature profile used in the design of the René 41 TPS (ref. 7) is shown in figure 2. A maximum surface temperature of about 2060°R is reached after 500 sec and is maintained for approximately 500 sec before decreasing to about 540°R at 2200 sec. The TPS is designed to restrict the temperature of the primary structure to 810°R. The maximum positive-differential design pressure during peak heating is approximately 0.68 psia; however, a higher differential design pressure (2.54 psia) occurs at much lower surface temperatures.

General description.- The 24- by 36-in. René 41 TPS model (fig. 3) is a shingled, radiative structure which features a corrugation-stiffened corrugated-skin heat shield, beaded fixed and flexible support ribs, and fibrous insulation. The heat-shield portion of the test model consists of full-sized test panel and a shortened fairing panel. Design details of the model are shown in figure 4. Table I shows the mass breakdown of the model. The actual mass of the TPS model is 1.491 lb/ft^2.

The geometry of the heat shield (corrugated skin and corrugated stiffener) is shown in figure 5. The corrugated skin is 0.008 in. thick and has a cross-sectional shape composed of a series of circular arc segments separated by flat segments. Lateral thermal expansion of the heat shield is restrained by the support ribs, and this expansion is accommodated by transverse displacement (an increase in depth) of the circular arc, resulting in negligible net growth in panel width and thus little effect on adjacent panels. The corrugated stiffeners are trapezoidal and had a thickness of 0.012 in. prior to chem-milling. However, to reduce the mass of the stiffeners, the sidewalls are chem-milled to 0.007 in. and the bottoms are sculptured to provide uniform response to stress. The sculptured (thicker) areas of the stiffeners are shown by the dark regions in figure 6. The corrugated skin is attached to the stiffeners by three independent rows of overlapping spot-welds along all the flat segments. Other design considerations of buckling, creep, and flutter of the corrugation were considered in the structural optimization (ref. 7).

Since the aerodynamic skin expands during heating, an expansion joint is required at one transverse edge of the heat-shield panel to permit relative motion of adjacent panels without allowing excessive ingress of the boundary-layer gases. (See fig. 4.) A shingle/slip-joint concept is used at the expansion joint, with the corrugated skins overlapping 0.63 in. Because adjacent skins are mounted at the same height, an interference of one skin thickness is used at the faying surface to minimize leakage.

The heat shield is supported 2.26 in. off the primary structure by two types of beaded support ribs (fig. 7). The ribs must transfer aerodynamic and heat-shield inertial loads to the primary structure and minimize heat conduction to the primary structure. A flexible rib (fig. 7(a)) allows for longitudinal expansion of the heat shield at the expansion joint. A fixed rib (fig. 7(b)) is used at the point where two adjacent panels butt. (See figs. 3 and 4.) Because the support ribs cannot

react to loads in the longitudinal (drag) direction, drag supports (fig. 7(b)) are located at 12-in. intervals along the fixed rib.

The support ribs are made up of a web and clips which attach the web to the heat shield and to the primary structure. Although the two types of ribs are functionally different, a common web design was developed to reduce costs. The details of the web and rib construction are given in figure 8. Web and clip thicknesses are 0.0067 in. and 0.030 in. The fixed and flexible ribs are attached to the heat shield and to the primary structure in the manner shown in figure 9. Bolts with a thermal insulation washer made of a glass-reinforced silicone laminate are used to attach support ribs to the primary structure. Blind rivets made of Haynes alloy No. 188[3] are used to attach the ribs to the heat shield.

Edge fairings (figs. 4 and 9(a)) were designed to seal the test specimen within the test cavity of the panel holder and to provide a smooth surface for the aerodynamic flow during testing. The forward and aft fairings were formed with corrugations identical to those used for the heat shield. The corrugations are closed out at one end to provide a smooth surface for the aerodynamic flow. The side fairings have flat flanges spot-welded to the heat shield. All the edge fairings are formed with a curved (half-circle) lip designed to support a braided ceramic rope-type seal (fig. 9(a)).

The insulation system (fig. 10) provides the main barrier to heat transfer from the hot shield to the primary structure. The insulating materials consist of 1.38 in. of Micro-Quartz and 0.60 in. of TG 15000 which are compressed by 10 percent to fit into the area between the heat shield and the primary structure. This 10-percent compression of the insulation has an insignificant effect on the thermal properties (ref. 7), provides better retention of the insulation blanket, and compensates for the slight shrinkage which occurs after repeated high-temperature exposures. A thin aluminum insulation restraint (fig. 9(a)) is used at the leading and trailing edges of the model to hold the insulation between the fixed ribs and the model edges in place. This restraint is not part of the actual TPS design. Additional thermal protection is provided by packing the expansion cavity between the flexible ribs with Micro-Quartz insulation; however, insulation is not placed between the corrugated stiffeners of the heat shield.

Instrumentation.- The model was instrumented with 64 thermocouples. The thermocouple locations are shown in figure 11 and table II. Eight 30-gage chromel-alumel fiberglass-insulated thermocouples were used to monitor the temperature of the aluminum primary structure. These thermocouples were attached to the primary structure with a high-temperature adhesive. Ceramo-chromel-alumel thermocouples were used on the heat shield, supports, and insulation. To evaluate temperature gradients throughout the insulation thickness, four thermocouples were distributed approximately 0.50 in. apart throughout the thickness at locations near the test panel center and near the flexible rib (see section A-A in fig. 11). To evaluate expansion joint leakage three thermocouples were attached longitudinally at three locations to the back side of the aerodynamic skin. The center thermocouple was expected to record a higher temperature if leakage should occur. The thermocouples on the heat shield and support structure were spot-welded to the structures. Motion-picture cameras were used for photographing the panel during the wind-tunnel tests, and still photography was used for recording model surface appearance throughout the test series.

---

[3]Haynes alloy No. 188: Registered trademark of Cabot Corp.

Panel Holder

The René 41 TPS model was mounted in a panel holder (figs. 12 and 13) which can accommodate test models up to 60.0 by 42.5 in. for wind-tunnel testing. (See refs. 8 and 9.) The aerodynamic surface of the panel holder was covered with a 1.0-in-thick low-conductivity Glasrock[4] fused silica panel which provided thermal protection for the internal structure. A sharp leading edge with a lateral row of spherical boundary-layer trips was used to promote a turbulent boundary layer, and aerodynamic fences provided uniform two-dimensional flow over the entire aerodynamic surface. Surface pressures and aerodynamic heating rates were varied by pitching the panel holder to a predetermined angle of attack.

The model was installed on the panel holder by bolting the aluminum primary structure to the sidewalls of the panel-holder interface system. Insulation washers were used to thermally isolate the model primary structure from the panel holder. The leading edge of the model was located 45 in. from the leading edge of the panel holder.

Facility

The TPS model was tested in the Langley 8-Foot High-Temperature Tunnel (fig. 14). This tunnel is a large blowdown facility that simulates aerodynamic heating and pressure loading at a nominal Mach number of 7 and altitudes between 80 000 and 130 000 ft. The high energy needed for this simulation is obtained by burning a mixture of methane and air under pressure in the combustor and expanding the products of combustion through a conical contoured nozzle into the free-jet test chamber. The flow enters a supersonic diffuser where an air ejector pumps it through a mixing tube and exhausts it to the atmosphere through a subsonic diffuser. This tunnel operates at a combustor total temperature $T_{t,c}$ from 2500°R to 3600°R, at free-stream dynamic pressures from 1.74 to 12.50 psia, and at free-stream Reynolds numbers from 0.3×10^6 to 2.2×10^6 per foot.

The test model is initially covered with acoustic baffles and stored in a pod below the test stream (fig. 14(b)) to protect it from adverse transient loads resulting from tunnel start-up. Once the desired flow conditions are established, the baffles are retracted and the model is rapidly inserted into the test stream on a hydraulically actuated elevator (fig. 14(c)). A model pitch system provides an angle-of-attack range of ±20°.

A radiant-heater system is used for both the radiant-heating tests and as a preheater for the aerothermal tests. This radiant-heater system consists of quartz-lamp radiators mounted under the acoustic baffles (fig. 14). The radiant lamps are powered by an ignition tube power supply and are controlled by a closed-loop servo system to produce the desired temperature histories. More detailed information concerning the test facility can be found in references 8 and 9.

Test Procedures and Data Reduction

The René 41 TPS model was subjected to radiant-heating tests and to radiant preheat/aerothermal-heating tests with the temperature-time history shown in

---

[4]Glasrock: Registered trademark of Glasrock Products, Inc.

figure 15. This temperature history is a simplified version of the design temperature profile shown in figure 2. In both the radiant-heating and the aerothermal-heating tests, radiant lamps were used to heat the model to the maximum operating temperature at a rate of 3.6°R/sec. The temperature profile was the same for both tests except that the aerothermal portion was deleted from the radiant tests and no radiant heating occurred after the aerothermal heating. All radiant heating occurred at atmospheric pressure.

Preliminary tests were conducted at low thermal loads to check the model and test equipment. The René 41 TPS model was then exposed to a total of 13 tests: 10 radiant-heating tests and 3 radiant preheat/aerothermal-heating tests. The maximum temperature and the time exposed to maximum temperature for each type of test are listed in table III. Incomplete radiant-heating tests are included to show exactly what conditions the model experienced. Table IV lists the pertinent wind-tunnel test conditions for two of the aerothermal-heating tests. The free-stream Mach number M_∞ was nominally 6.7, the combustor total temperature was approximately 3250°R, and the approximate Reynolds number was 1.4×10^6 per foot. The free-stream dynamic pressures were 8.4 and 9.1 psia.

Several events subjected the model to unusual load conditions. During test 2, the model supports were crushed by a severe breakdown of flow during a tunnel checkout run which was conducted concurrently with the radiant-heating test. However, the model was completely repaired and testing was continued. During tests 3, 4, and 5, equipment failure caused the radiant heaters to turn off before maximum temperature was attained. The model was damaged beyond repair during test 11 when a second breakdown of flow occurred when the model was inserted in the test section. Two additional aerothermal tests were made on the damaged model to test the TPS damage tolerance. These tests are discussed in greater detail in the "Results and Discussion" section.

During most of the tests, the temperature of the heat shield was raised to the maximum operating temperature (2060°R) by using the radiant heaters at atmospheric pressure. For the radiant-heating tests (fig. 15), the maximum surface temperature was maintained for periods up to approximately 500 sec and then was allowed to follow the remainder of the expected Space Shuttle trajectory until the natural cooling rate was less than 3.6°R/sec. For the radiant preheat/aerothermal-heating tests (fig. 15), the maximum preheating temperature was maintained for approximately 500 sec prior to wind-tunnel exposure in order to expose the heat shield to aerodynamics loads at the heat shield's maximum temperature. However, the aerothermal-heating exposure could be programmed to occur at any point during the simulated Space Shuttle trajectory. When wind-tunnel flow conditions capable of maintaining the desired temperature were stabilized, the model was quickly exposed to the hypersonic stream for as long as test conditions could be maintained. (See table III.)

The procedure for the aerothermal part of the tests was to start the tunnel, obtain correct flow conditions, deenergize the radiant heaters, retract the heaters and acoustic baffles, and insert the model into the hypersonic stream while simultaneously pitching the panel holder. The desired angle of attack was obtained prior to reaching the stream centerline. At the end of the aerothermal exposure, this procedure was reversed. The tunnel shutdown was initiated after the heaters and the acoustic baffles had covered the model and the heaters had been reenergized. Although the heaters were programmed to continue to follow the cool-down trajectory until the natural cooling rate was less than 3.6°R/sec, operational problems prevented the heaters from being reenergized. The time between the lamps being deenergized and the model entering the stream was kept to a minimum (approximately 5 sec).

Model and tunnel instrumentation data were recorded with high-speed digital recorders. During radiant-heating tests and preheating events, thermocouple outputs were recorded at 2-sec intervals. During the aerothermal-heating portion of the tests, data were recorded at 20 samples per second. All data were reduced to engineering quantities at the Langley Central Digital Data Recording Subsystem. The analytical quantities reported for these wind-tunnel tests are based on the thermal, transport, and flow properties of the test medium of the combustion products as determined from reference 10. Free-stream conditions in the test section were determined from reference measurements in the combustor by using results from tunnel-stream-survey tests such as those reported in reference 8. The local Mach number was obtained from oblique-shock relations.

RESULTS AND DISCUSSION

Results of the René 41 TPS model tests are summarized in tables III and IV. The model was held at its approximate maximum operating temperature (2060°R) by radiant heaters for a total of 63.7 minutes and was exposed to a hypersonic stream for a total of 53 sec.

TPS Structural Performance

Structural ruggedness of the TPS was demonstrated during the test series when the model was inadvertently subjected to the previously mentioned unusual load conditions. During test 2, when the severe breakdown of flow occurred during a tunnel checkout, the model supports were crushed. Damage was confined to one side of the flexible rib. The damage included a bent web and broken and pulled-out spot-welds. There was no damage to the heat shield. The model was fully repaired with spare parts and testing was continued. However, during test 11 (attempted radiant preheat/aerothermal test) flow breakdown occurred upon model insertion and a panel separated from the front end of the panel holder and crushed the TPS model. The panel consisted of Glasrock tiles bonded to a steel plate which was bonded to the panel holder. The sequence of events is shown in figure 16. Damage to the model was extensive and included a large indentation across the middle of the test heat shield as well as one major and several minor penetrations (fig. 17). Insulation was sucked out in the immediate area of the major penetration (fig. 17(b)). To evaluate the effect this damage would have on a metallic TPS in a hypersonic stream, the damaged René 41 TPS model was exposed to two radiant preheat/aerothermal tests. The major penetration was covered with insulation to prevent the radiant preheat portion of the tests from overheating the aluminum primary structure prior to the aerothermal exposure. The insulation was placed over the penetration during the radiant preheat portion so that upon model insertion into the test stream the insulation would be blown away. Also, after the aerothermal exposure the model was allowed to cool naturally. After the two radiant preheat/aerothermal tests totaling 53 sec of aerothermal exposure (fig. 18), the only noticeable difference was a darkening of the René 41 heat shield and the aluminum primary structure around the major penetration. No structural deterioration could be seen. These tests demonstrated the ruggedness of a severely damaged metallic TPS. The primary structure became hotter than the 810°R design limit during the very short aerothermal exposure time, but there was no catastrophic damage. If similar impact damage had occurred on an RSI TPS, more impact damage would have been expected. Also, additional damage would be expected because of erosion of the RSI, as shown in reference 11.

TPS Thermal Performance

The temperature distributions on the heat shield, through the insulation, and on the primary structure for both a radiant-heating test and a radiant preheat/aerothermal-heating test are shown in figure 19. For the radiant-heating test, the heat-shield skin reached a temperature of 2050°R with a slightly lower temperature for the bottom surface of the corrugated stiffener. The maximum temperature in the insulation was 1970°R. The temperature of the primary structure away from the support ribs only reached 780°R, which is 30°R less than the design value of 810°R. The design value is based on the assumption that there is no heat loss from the backface of the primary structure (i.e., it is an adiabatic surface). If we assume that there were some losses from the backface of the primary structure along with the reduced heat input to the model, the TPS performed essentially as expected. The only temperature distributions measured in the insulation under radiant preheat/aerothermal conditions (fig. 19(b)) were measured after the test heat shield of the model had been damaged. The temperature of the heat shield (thermocouples (TC's) 36 and 60) was 2050°R, the same as for the radiant-heating-only test; however, the temperature in the insulation was much higher than for the radiant-heating-only test. At an insulation depth of 1.0 in. from the primary structure (TC 40) the temperature reached 1780°R, 337°R higher than for the radiant-heating-only test (fig. 19(a)). Also, the thermocouple 0.5 in. above the primary structure (TC 41) was 266°R higher when exposed to the radiant preheat/aerothermal conditions than for radiant heating only. Thermocouple 42, on the primary structure, was damaged earlier in the test series. These higher temperatures in the insulation probably resulted from the lateral indentation near the center of the test panel significantly compressing the insulation. An enlargement of the aerothermal portion of the test is shown on the right side of figure 19(b). This enlargement illustrates the thermal responses caused by each of the tunnel events. Even though the insulation temperatures were higher than in the radiant-heating-only test (fig. 19(a)), the slow increase in insulation temperature at approximately 9.0 in. from the center of the major penetration (TC's 40 and 41), indicates hot gas ingress had no noticeable effect on the insulation temperatures.

The temperature response of the heat shield, the support, and the primary structure are shown in figure 20. For a radiant-heat-only test, the heat-shield-skin temperature at this leading-edge location (TC 2) was 2030°R, approximately equal to the desired temperature (2060°R). The maximum upper clip temperature (TC 3) was 1966°R and the maximum primary-structure temperature (TC 5) was 820°R. The primary-structure temperature at TC 5 was 40°R higher than the primary-structure temperature at TC 42, which was located approximately 10 in. from the flexible support rib. This temperature difference indicates a small amount of heat conduction down the support structure. The temperature response of the heat shield, the support web, and the primary structure for a radiant preheat/aerothermal test are shown in figure 20(b). The heat-shield-skin temperature was lower than expected in this area (1930°R), indicating the heating from the radiant heaters was not evenly distributed over the mode surface for this run. Therefore, all other temperatures on the model were lower. The sudden temperature increase for TC 4 indicates the damaged edge fairing may have allowed ingress of a small amount of hot gas.

The temperature response of the heat shield and the primary structure in the vicinity of the major penetration during a radiant preheat/aerothermal test are shown in figure 21. During the radiant preheat portion of the test the penetration was covered with insulation, but the insulation was allowed to be blown off during the aerothermal exposure. The temperature of the 0.090-in-thick aluminum primary structure (TC 64) directly underneath the major penetration reached 1120°R. As can be

seen from the expanded time scale, this temperature was slightly higher than the temperature at a location about 6 in. upstream (TC 45) until the model was exposed to the test stream. During the exposure, the temperature for TC 64 rose very rapidly while the temperature for TC 45 increased at a much slower rate. The internal heating rate corresponding to the maximum temperature-rise rate for TC 64 was 4.6 Btu/ft^2-sec. If we adjust this heating rate to a cold-wall value by assuming a constant adiabatic temperature in the penetration cavity, the cold-wall heating rate of the primary structure represents 32 percent of the potential cold-wall heating of the heat shield exterior. Thermocouple 45 reached a temperature of 820°R (only 10° higher than design). The aerothermal portion of the test was 32 sec. During these tests, the damaged area did not enlarge; however, the high internal heating directly to the primary structure indicates that had the damaged area been exposed to aerodynamic heating for the entire trajectory, an aluminum burn-through would have occurred. The severity of a burn-through would depend on its location on a vehicle. When the model was damaged in the wind-tunnel test, the fibrous insulation in the damaged area was immediately sucked out. The damage tolerance of the TPS could be improved by packaging the insulation so that it would remain at least partially intact when the penetration damage to the heat shield occurs, thereby lowering the primary-structure temperature and preventing or delaying a burn-through.

CONCLUDING REMARKS

A flight-weight, metallic thermal protection system (TPS) model applicable to Earth-entry and hypersonic-cruise vehicles was subjected to multiple cycles of both radiant and aerothermal heating in order to evaluate its aerothermal performance, structural integrity, and damage tolerance. The TPS is a mass-optimized (1.491 lb/ft^2), shingled, radiative structure constructed of René 41, a nickel-base alloy. The TPS is designed for a maximum operating temperature of 2060°R and features a shingled, corrugation-stiffened corrugated-skin heat shield with insulation and beaded support ribs.

The TPS model was evaluated in the Langley 8-Foot High-Temperature Tunnel. The model was subjected to 10 radiant-heating tests, and to 3 radiant preheat/aerothermal-heating tests (representative of a Space Shuttle entry temperature history, or trajectory). The aerothermal tests were conducted at a nominal free-stream Mach number of 6.7, a stagnation temperature of approximately 3250°R, and a Reynolds number of approximately 1.4×10^6 per foot. The model outer surface was maintained at the approximate maximum operating temperature of 2060°R for a total of 63.7 minutes and was exposed to a hypersonic stream for a total of 53 sec.

Under radiant heating conditions with a maximum surface temperature of 2050°R, the TPS limited the primary structure away from the support ribs to temperatures below 780°R, which is 30°R less than the design temperature of 810°R. Thermal performance was as expected over the 10 radiant-heating cycles, although the temperatures were not corrected for heat loss out the backface of primary structure to the cooler panel-holder cavity.

During the first attempt at an aerothermal exposure, a failure in the panel-holder test fixture severely damaged the model. However, two radiant preheat/aerothermal tests were made with the damaged model to test its damage tolerance. In general, interior temperatures around the damaged area were higher than those in the radiant-heating tests. The aluminum primary structure reached 1120°R directly under the penetration during the aerothermal exposure, and the aluminum became discolored in that localized area; however, no structural deterioration could be seen. About

6 in. upstream from the damage, the primary structure reached 820°R, 10°R higher than the design limit. During the two radiant preheat/aerothermal tests, the penetration-damaged area did not enlarge; however, the rapidly increasing structural temperature measured during these tests indicates that had the damaged area been exposed to aerodynamic heating for the entire trajectory, an aluminum burn-through would have occurred. The severity of a burn-through would depend on its location on a vehicle. When the model was damaged in the wind-tunnel test, the fibrous insulation in the damaged area was immediately sucked out. The damage tolerance of the TPS could be improved by packaging the insulation so that it would remain at least partially intact when the penetration damage to the heat shield occurs, thereby lowering the primary-structure temperature and preventing or delaying a burn-through.

Langley Research Center
National Aeronautics and Space Administration
Hampton, VA 23665
May 16, 1984

REFERENCES

1. Sawyer, James Wayne: Aerothermal and Structural Performance of a Cobalt-Base Superalloy Thermal Protection System at Mach 6.6. NASA TN D-8415, 1977.

2. Deveikis, William D.; Miserentino, Robert; Weinstein, Irving; and Shideler, John L.: Aerothermal Performance and Structural Integrity of a René 41 Thermal Protection System at Mach 6.6. NASA TN D-7943, 1975.

3. Bohon, Herman L.; Sawyer, J. Wayne; Hunt, L. Roane; and Weinstein, Irving: Performance of Thermal Protection Systems in a Mach 7 Environment. J. Spacecr. & Rockets, vol. 12, no. 12, Dec. 1975, pp. 744-749.

4. Bohon, Herman L.; Shideler, John L.; and Rummler, Donald R.: Radiative Metallic Thermal Protection Systems: A Status Report. J. Spacecr. & Rockets, vol. 14, no. 10, Oct. 1977, pp. 626-631.

5. Kelly, H. Neale; Rummler, Donald R.; and Jackson, L. Robert: Research in Structures and Materials for Future Space Transportation Systems - An Overview. J. Spacecr. & Rockets, vol. 20, no. 1, Jan.-Feb. 1983, pp. 89-96.

6. Emde, Wendall D.: Thermal Protection System for the Shuttle Orbiter. Bicentennial of Materials Progress, Volume 21 of National SAMPE Symposium and Exhibition, Soc. Advance. Mater. & Process Eng., 1976, pp. 964-978.

7. Varisco, Angelo; Bell, Paul; and Wolter, Willy: Design and Fabrication of Metallic Thermal Protection Systems for Aerospace Vehicles. NASA CR-145313, 1978.

8. Deveikis, William D.; Bruce, Walter E., Jr.; and Karns, John R.: Techniques for Aerothermal Tests of Large, Flightweight Thermal Protection Panels in a Mach 7 Wind Tunnel. NASA TM X-71983, 1974.

9. Deveikis, William D.; and Hunt, L. Roane: Loading and Heating of a Large Flat Plate at Mach 7 in the Langley 8-Foot High-Temperature Structures Tunnel. NASA TN D-7275, 1973.

10. Leyhe, E. W.; and Howell, R. R.: Calculation Procedure for Thermodynamic, Transport, and Flow Properties of the Combustion Products of a Hydrocarbon Fuel Mixture Burned in Air With Results for Ethylene-Air and Methane-Air Mixtures. NASA TN D-914, 1962.

11. Hunt, L. Roane: Aerodynamic Heating in Large Cavities in an Array of RSI Tiles. NASA TN D-8400, 1977.

TABLE I.- COMPONENT MASS OF RENÉ 41 TPS MODEL

Element	Mass, lb/ft^2	Element percent of TPS
Surface panel:		
Skin	0.3600	24.1
Stiffener	.4800	32.2
Doublers	.0103	.7
Attach rivets	[a].0240	1.6
Supports:		
Webs	.0324	2.2
Upper clips	.0570	3.8
Lower clips	.0306	2.1
Drag brackets	.0149	1.0
Attach hardware	[a].0302	2.0
Insulation:		
Micro-Quartz	[a].4020	27.0
TG 15000	[a].0500	3.4
Total	1.4914	100

[a]Estimated.

TABLE II.- THERMOCOUPLE LOCATIONS

Thermocouple no.	Row-column[a]	Location	Thermocouple no.	Row-column[a]	Location
1	4-1	Edge seal, fairing heat-shield panel	33	4-10	Stiffener bottom, test heat-shield panel
2	4-2	Skin, fairing heat-shield panel	34	1-11	Edge seal, test heat-shield panel
3	4-2	Clip, fairing heat-shield panel	35	2-11	Skin, test heat-shield panel
4	4-2	Standoff web, fairing heat-shield panel	36	4-11	Skin, test heat-shield panel
5	4-2	Primary structure, fairing heat-shield panel	37	4-11	Stiffener bottom, test heat-shield panel
6	2-3	Skin, fairing heat-shield panel	38	4-11	Insulation at 1.8 in., test heat-shield panel
7	4-3	Skin, fairing heat-shield panel	39	4-11	Insulation at 1.5 in., test heat-shield panel
8	6-3	Skin, fairing heat-shield panel	40	4-11	Insulation at 1.0 in., test heat-shield panel
9	4-5	Clip, fairing heat-shield panel	41	4-11	Insulation at 0.5 in., test heat-shield panel
10	4-5	Standoff web, fairing heat-shield panel	42	4-11	Primary structure, test heat-shield panel
11	4-5	Primary structure, fairing heat-shield panel	43	6-11	Skin, test heat-shield panel
12	2-6	Skin, fairing heat-shield panel	44	6-11	Stiffener bottom, test heat-shield panel
13	4-6	Skin, fairing heat-shield panel	45	6-11	Primary structure, test heat-shield panel
14	6-6	Skin, fairing heat-shield panel	46	7-11	Edge seal, test heat-shield panel
15	6-6	Clip, fairing heat-shield panel	47	4-13	Skin, test heat-shield panel
16	6-6	Standoff web, fairing heat-shield panel	48	4-13	Stiffener bottom, test heat-shield panel
17	6-6	Primary structure, fairing heat-shield panel	49	4-16	Skin, test heat-shield panel
18	2-7	Skin, test heat-shield panel	50	4-16	Clip, test heat-shield panel
19	4-7	Skin, test heat-shield panel	51	4-16	Standoff web, test heat-shield panel
20	6-7	Skin, test heat-shield panel	52	4-16	Primary structure, test heat-shield panel
21	2-8	Skin, test heat-shield panel	53	4-17	Edge seal, test heat-shield panel
22	2-8	Clip, test heat-shield panel	54	2-4	Skin, fairing heat-shield panel
23	2-8	Standoff web, test heat-shield panel	55	4-4	Skin, fairing heat-shield panel
24	2-8	Primary structure, test heat-shield panel	56	5-3	Skin, fairing heat-shield panel
25	4-8	Skin, test heat-shield panel	57	6-4	Skin, fairing heat-shield panel
26	6-8	Skin, test heat-shield panel	58	2-12	Skin, test heat-shield panel
27	4-9	Insulation at 1.8 in., test heat-shield panel	59	3-11	Skin, test heat-shield panel
28	4-9	Insulation at 1.5 in., test heat-shield panel	60	4-12	Skin, test heat-shield panel
29	4-9	Insulation at 1.0 in., test heat-shield panel	61	6-12	Skin, test heat-shield panel
30	4-9	Insulation at 0.5 in., test heat-shield panel	62	4-14	Skin, test heat-shield panel
31	4-9	Primary structure, test heat-shield panel	63	4-15	Skin, test heat-shield panel
32	4-10	Skin, test heat-shield panel	[b]64	6-13	Primary structure, test heat-shield panel

[a]See figure 11.
[b]Added after model damage.

TABLE III.- SUMMARY OF TESTS

Test	Type of test	Maximum radiant temperature (av), °R	Maximum aerothermal temperature (av), °R	Time at maximum surface temperature, sec, for -	
				Radiant test	Aerothermal test
1	Radiant	2030		34	
2	Radiant[a]	2050		554	
3	Radiant	709		[b]0	
4	Radiant	1623		[b]0	
5	Radiant	689		[b]0	
6	Radiant	2000		14	
7	Radiant	2099		542	
8	Radiant	2095		554	
9	Radiant	1983		[b]0	
10	Radiant	2100		574	
11	Aerothermal[c]	2100		562	
12	Aerothermal	2035	2063	547	21
13	Aerothermal	1990	1940	440	32

[a]Model damaged when flow broke down during tunnel checkout.
[b]Equipment failure caused radiant heaters to turn off (rapid cool downs).
[c]Model damaged when flow broke down on model insertion.

TABLE IV.- WIND-TUNNEL TEST CONDITIONS

Test	$T_{t,c}$, °R	α, deg	q_∞, psia	M_∞	M_ℓ	R, per foot
12	3340	11.1	8.4	6.7	4.9	1.338×10^6
13	3160	12.4	9.1	6.6	4.6	1.430

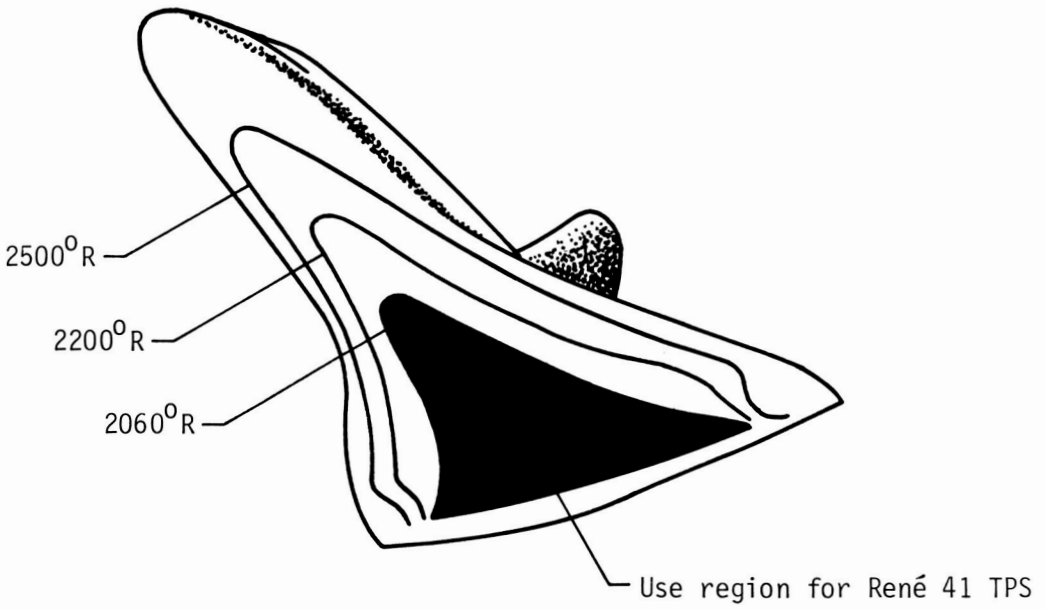

Figure 1.- Entry isotherms on lower surface of Space Shuttle orbiter.

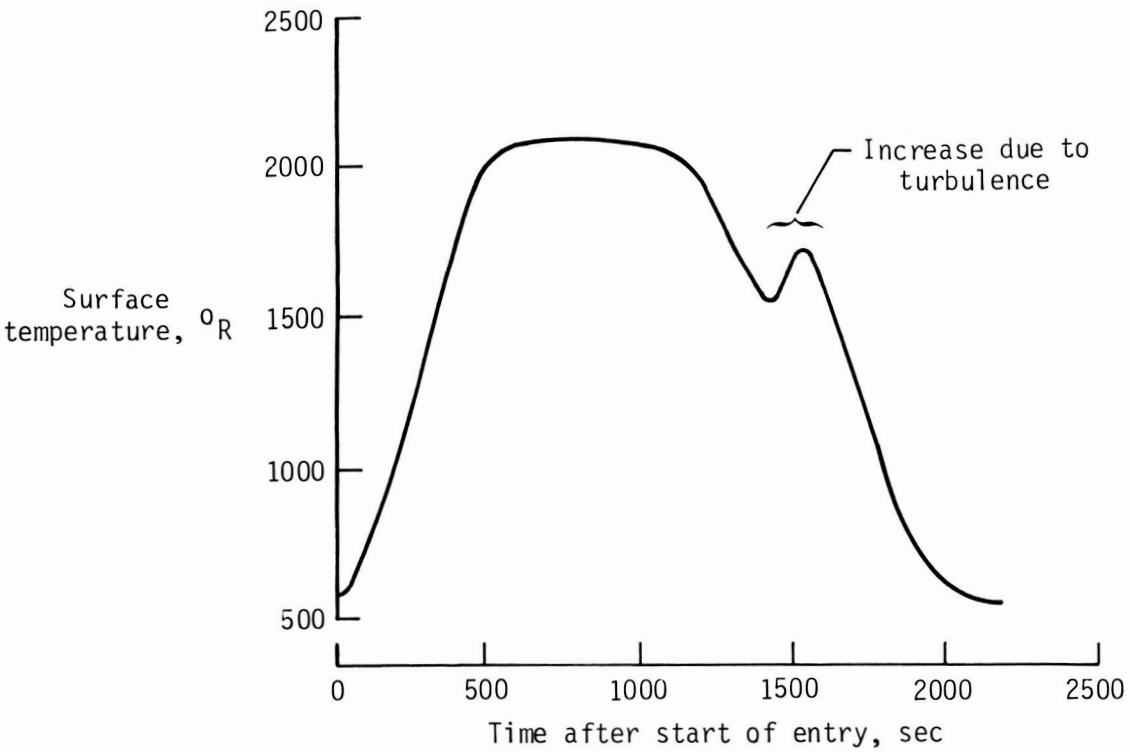

Figure 2.- Temperature history of René 41 for Space Shuttle entry trajectory (ref. 7).

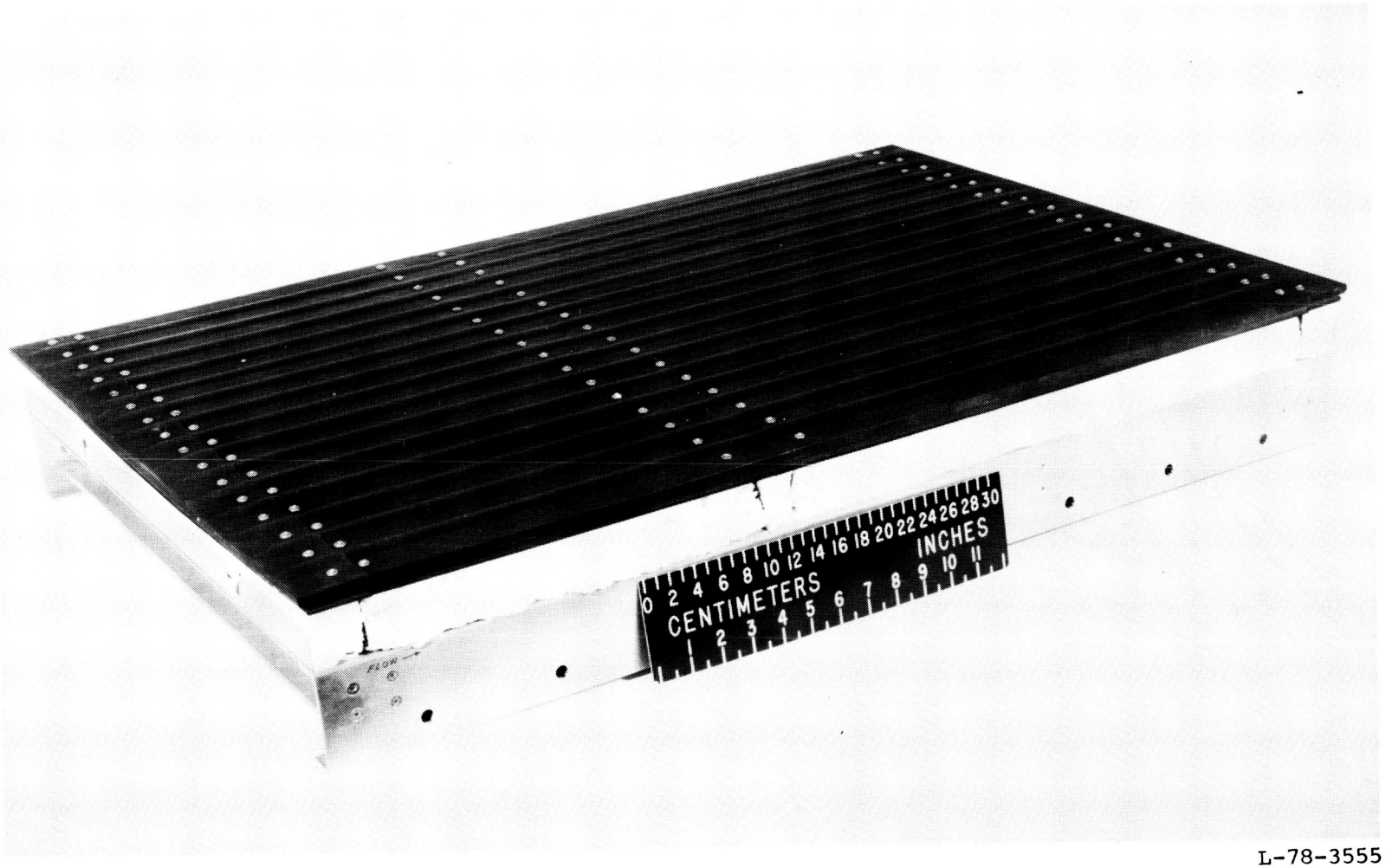

L-78-3555

Figure 3.- René 41 thermal protection system model.

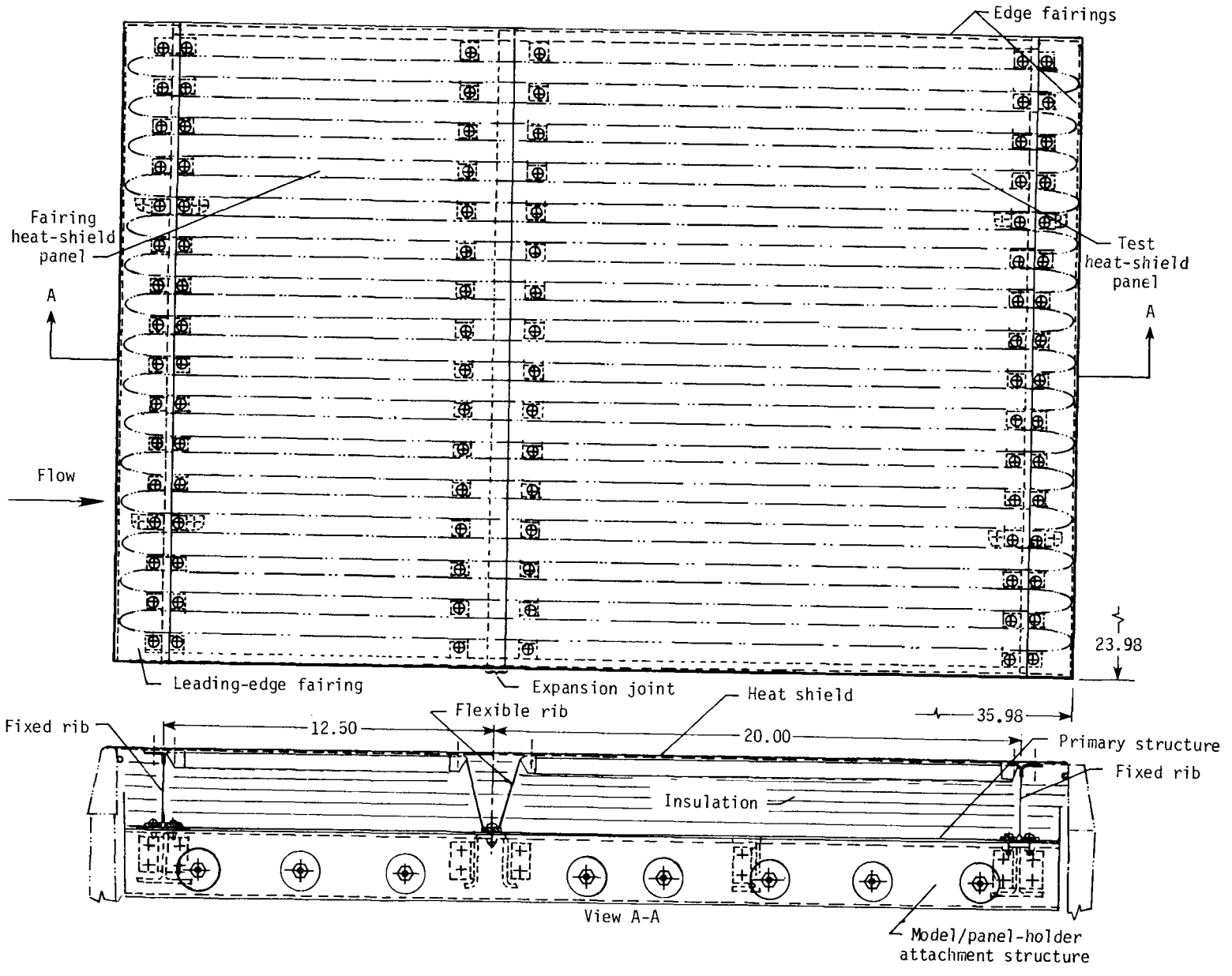

Figure 4.- Design details of TPS model. Dimensions are in inches.

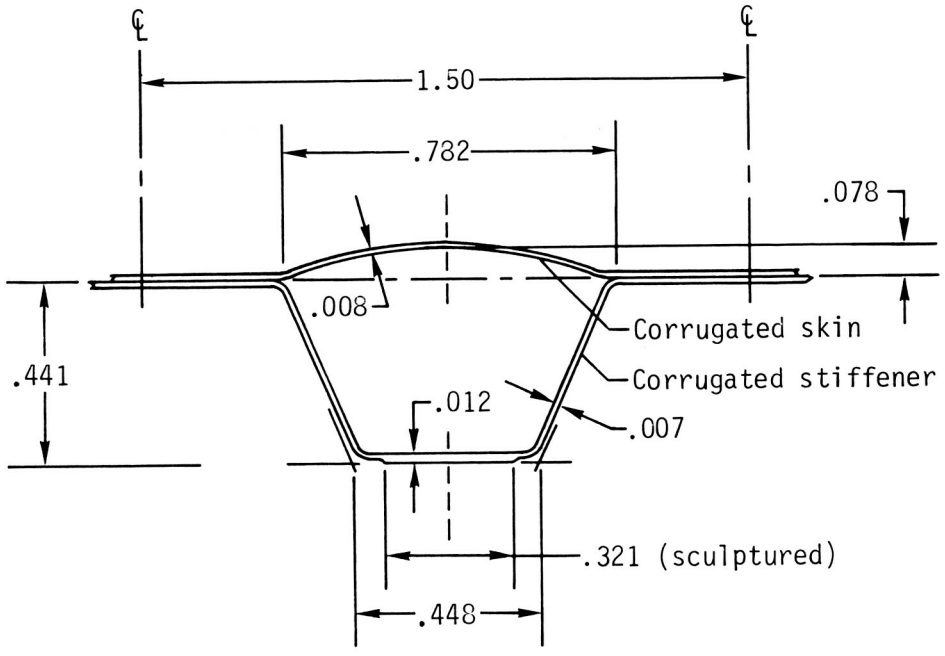

Figure 5.- Geometry of heat shield. Dimensions are in inches.

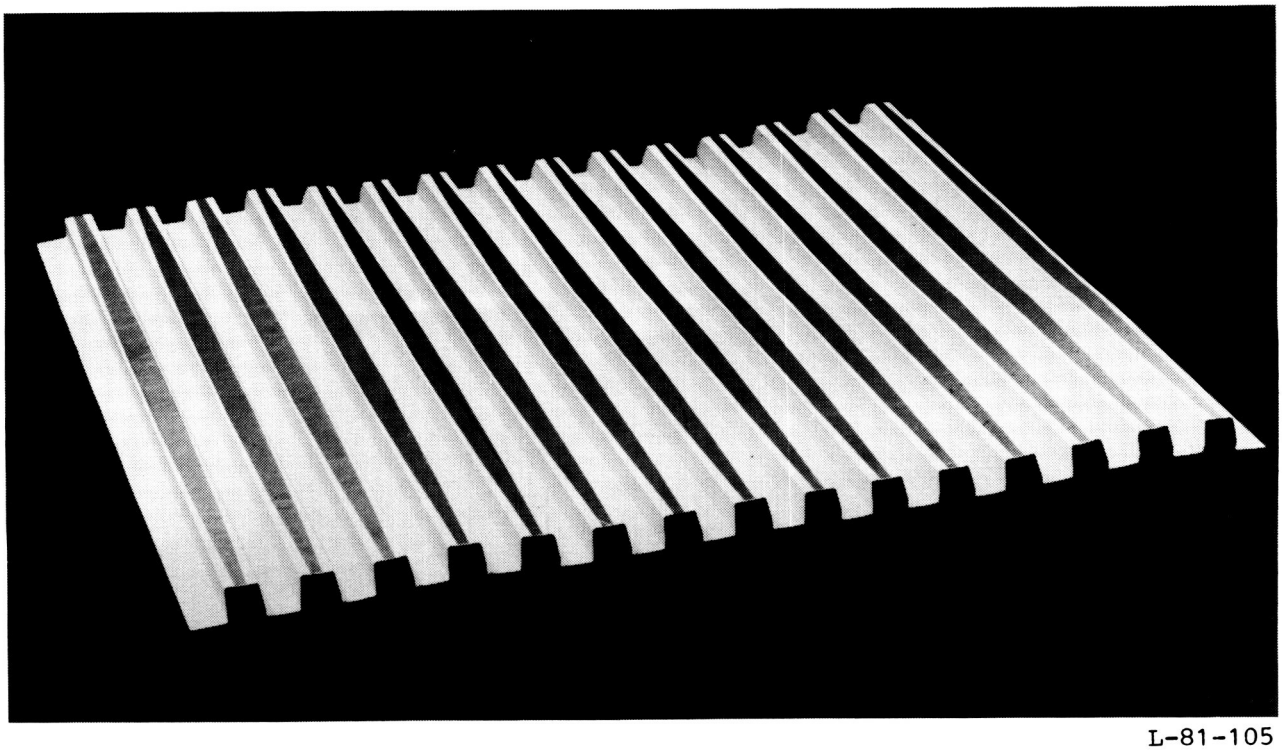

L-81-105

Figure 6.- Sculptured corrugated stiffener. (Sculptured areas are indicated by darker regions.)

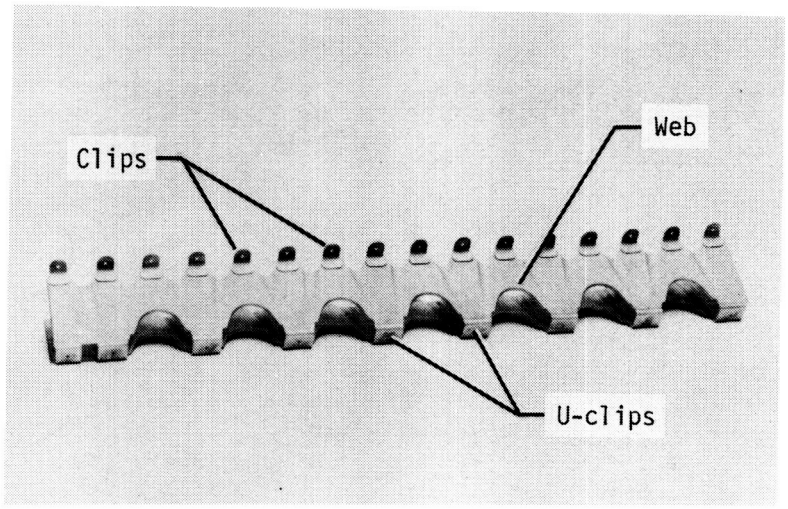

(a) Flexible rib.

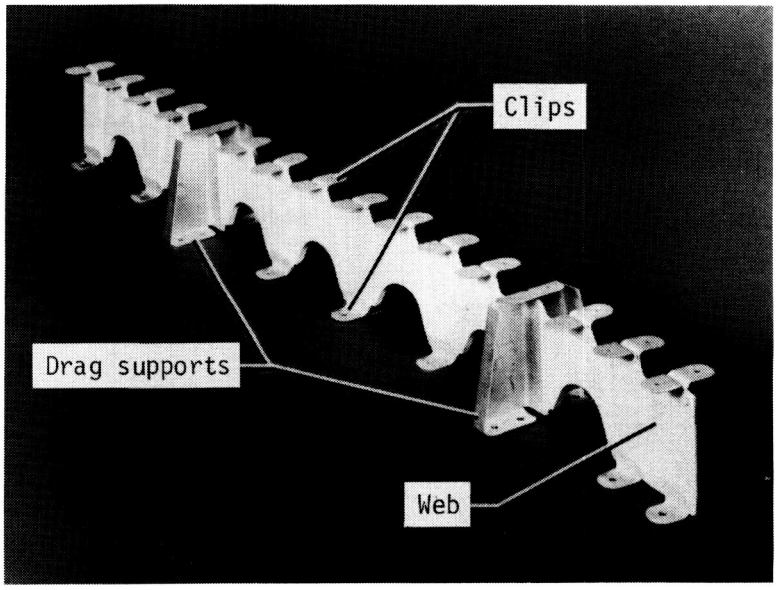

(b) Fixed rib with drag supports.

L-84-44

Figure 7.- Beaded support ribs.

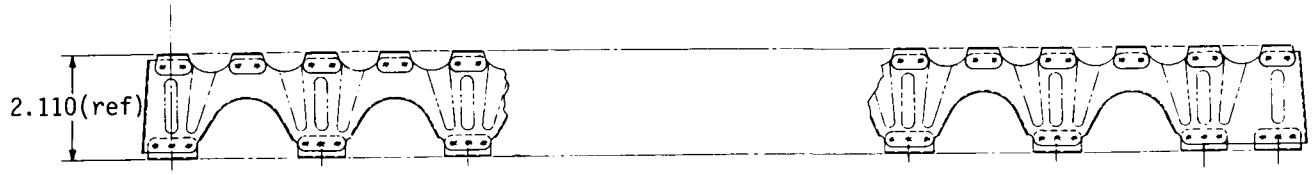

(a) Details of flexible rib.

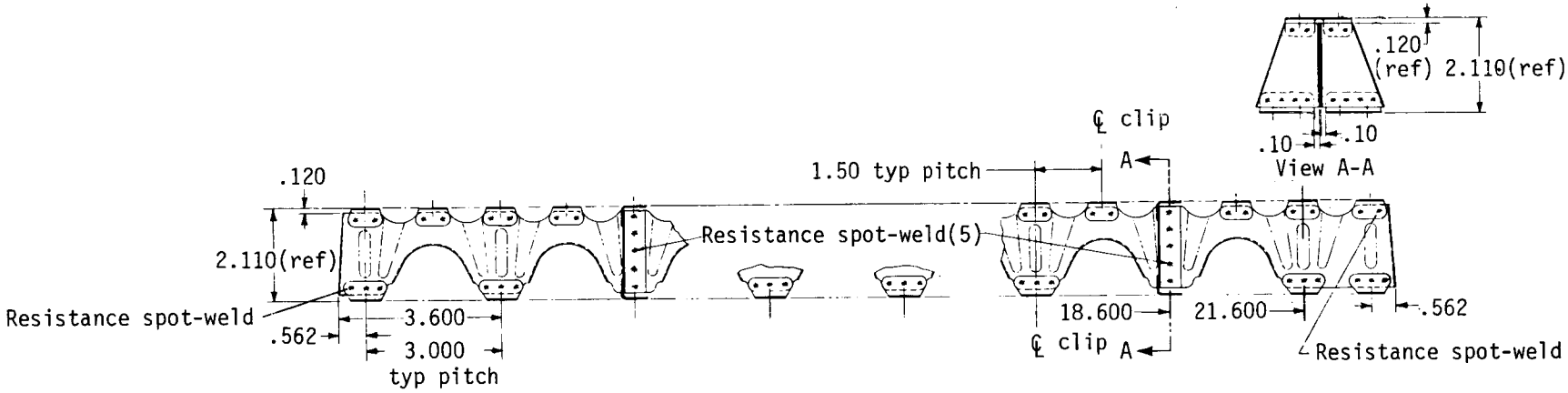

(b) Details of fixed rib.

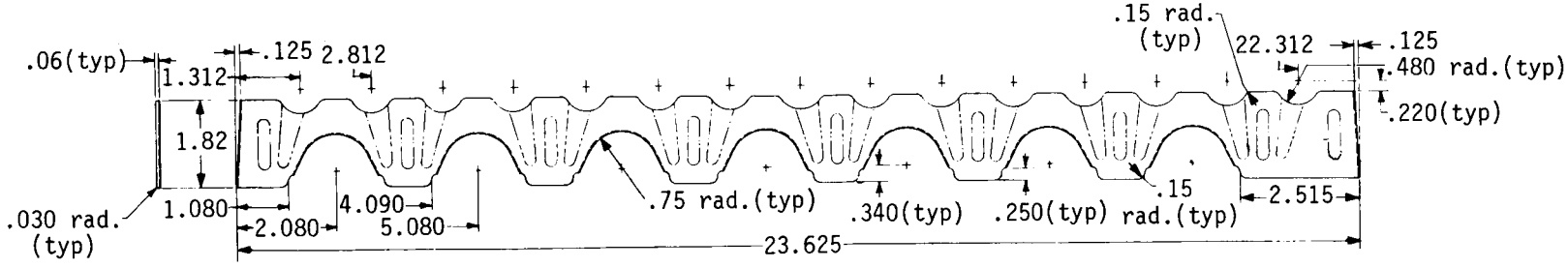

(c) Details of web.

Figure 8.- Details of web and rib construction. Dimensions are in inches.

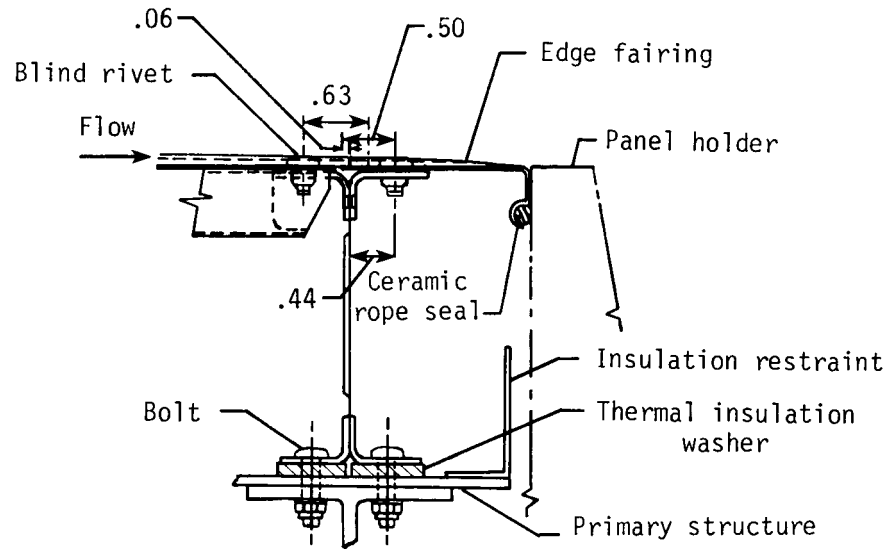

(a) Fixed rib.

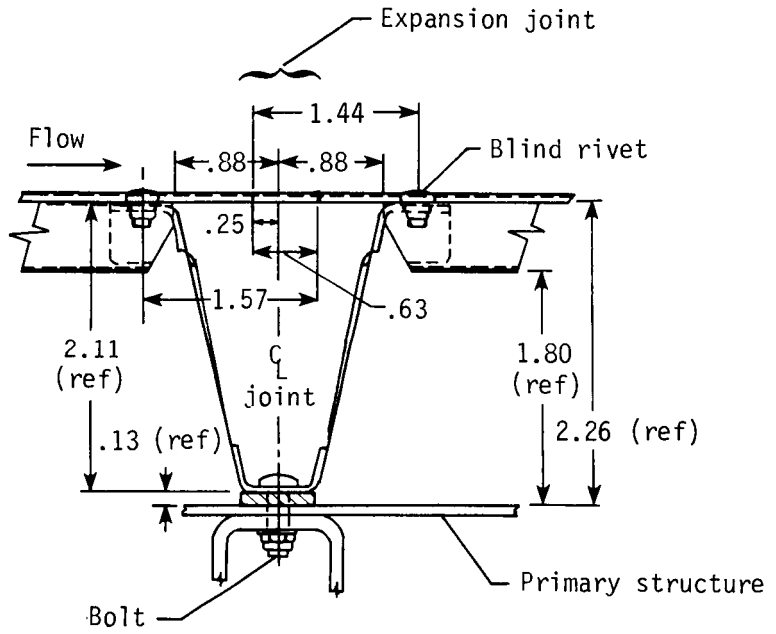

(b) Flexible rib.

Figure 9.- Details of support attachment. Dimensions are in inches.

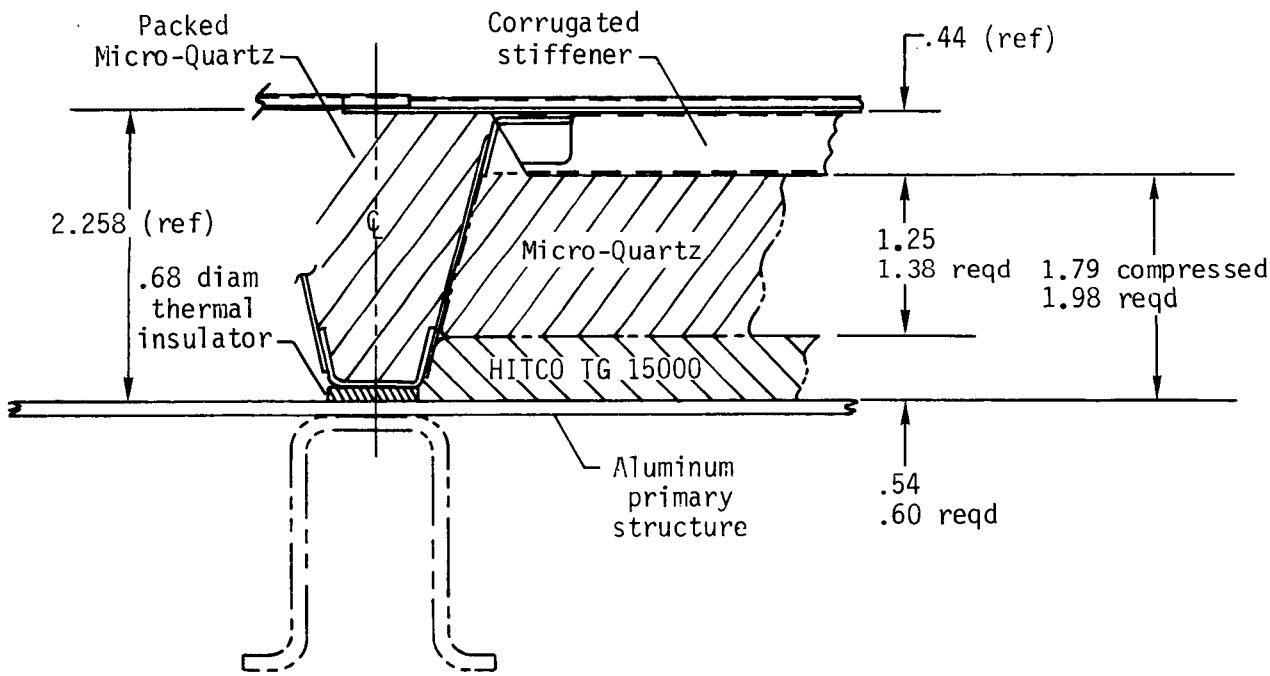

Figure 10.- Insulation system. Dimensions are in inches.

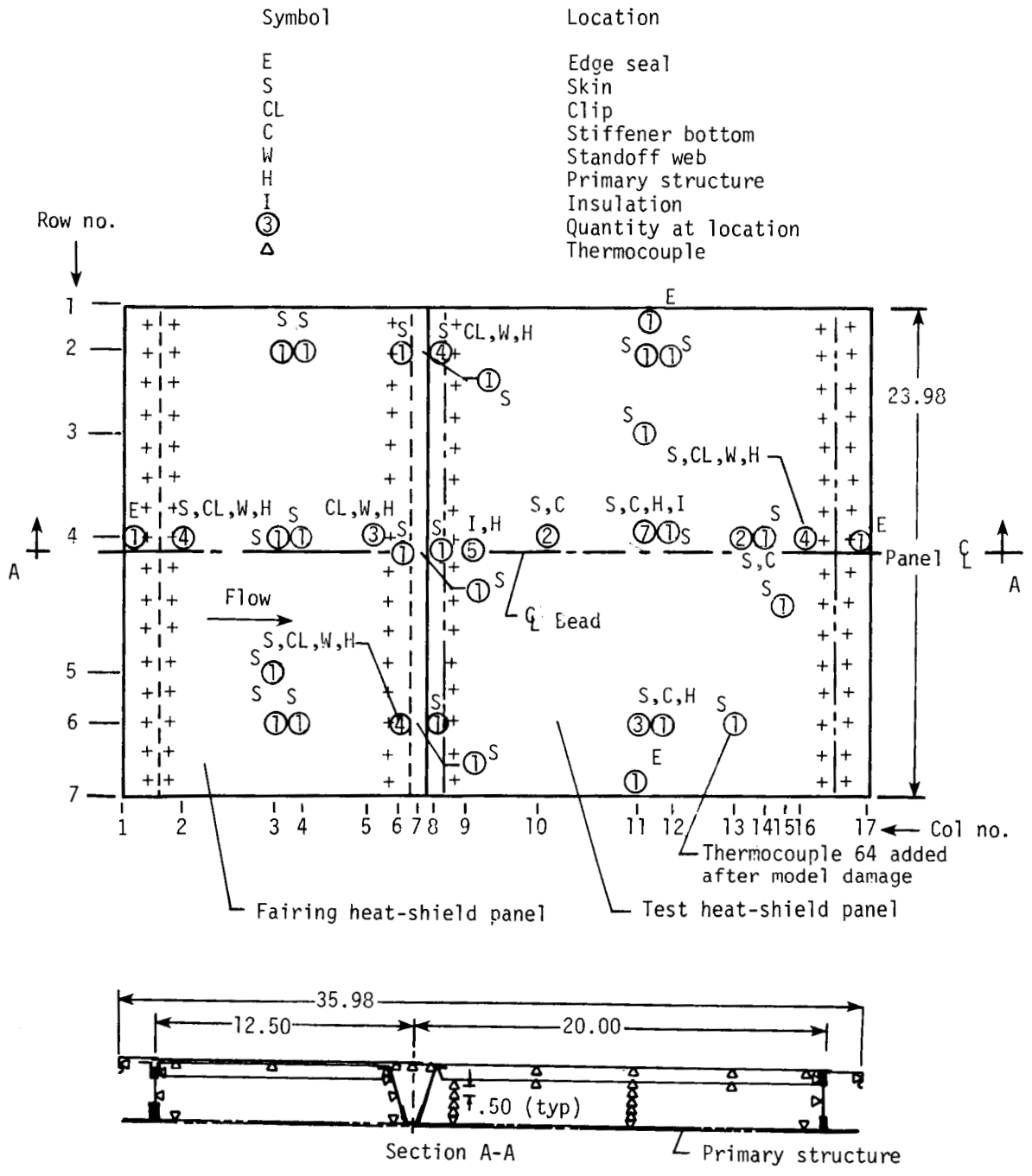

Figure 11.- Instrumentation for René 41 TPS model. Dimensions are in inches.

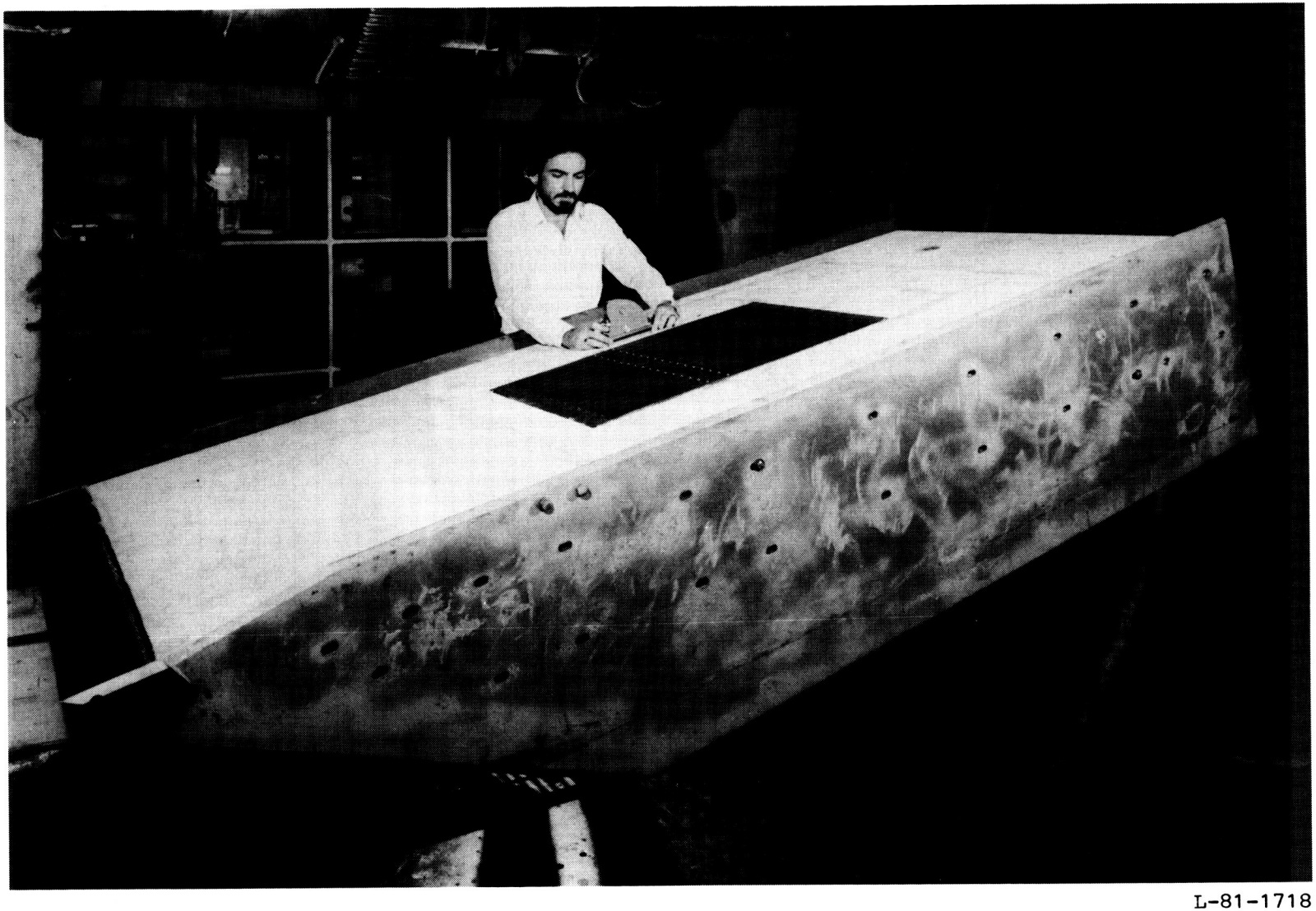

L-81-1718

Figure 12.- Panel holder (with René 41 TPS model installed) in Langley 8-Foot High-Temperature Tunnel.

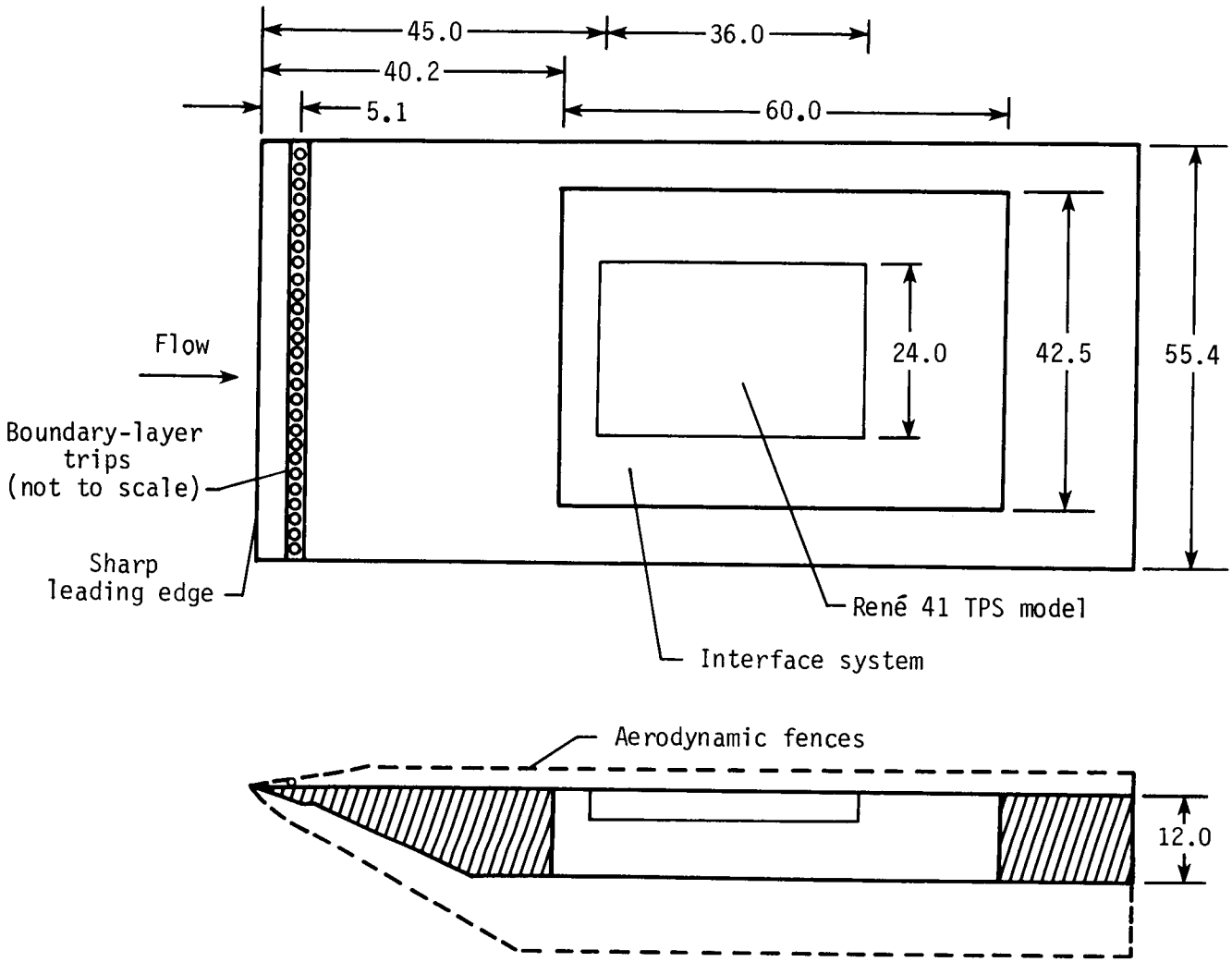

Figure 13.- Sharp-leading-edge panel holder with TPS model installed. Dimensions are in inches.

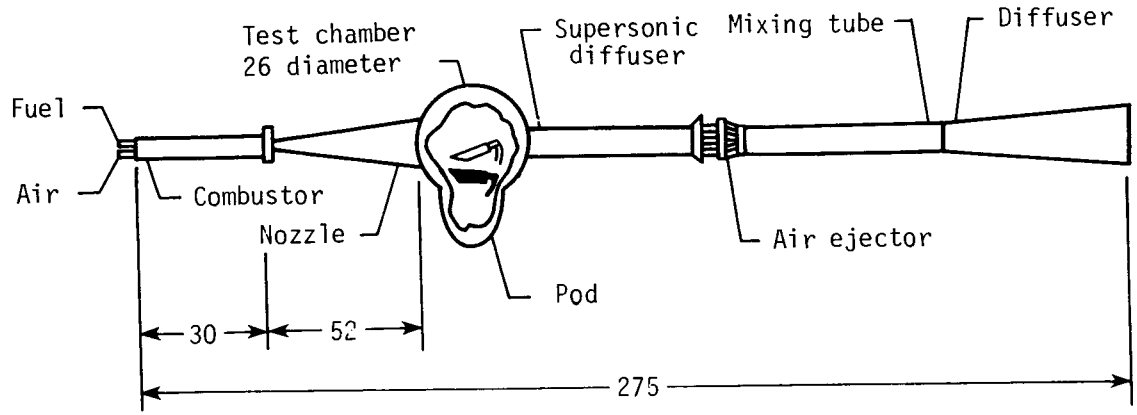

(a) Schematic of tunnel.

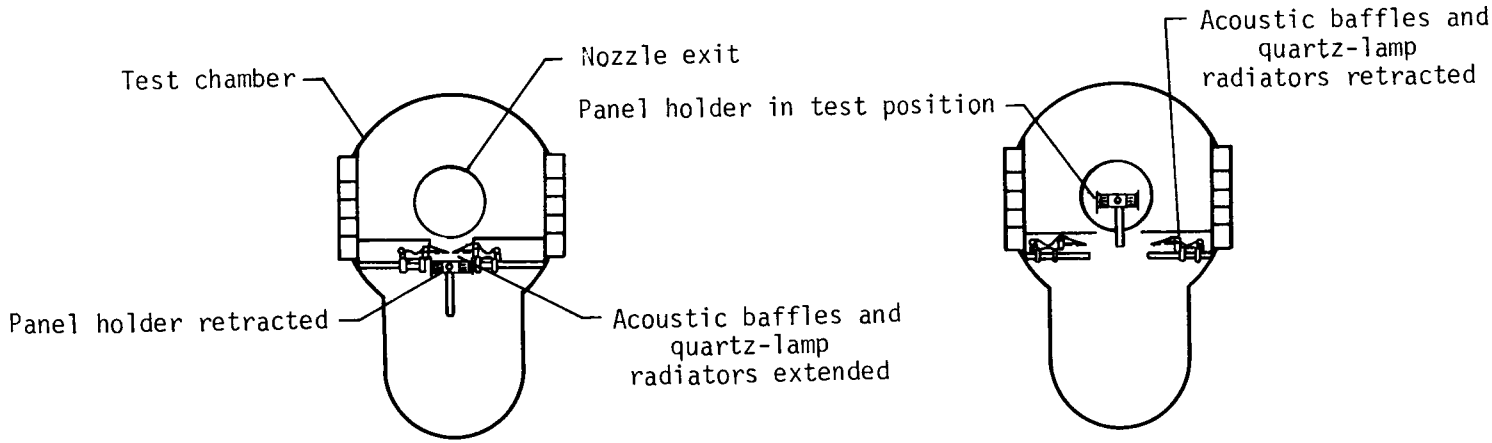

(b) Model position during preheat.

(c) Model position during test.

Figure 14.- Schematic of Langley 8-Foot High-Temperature Tunnel. Dimensions are in feet.

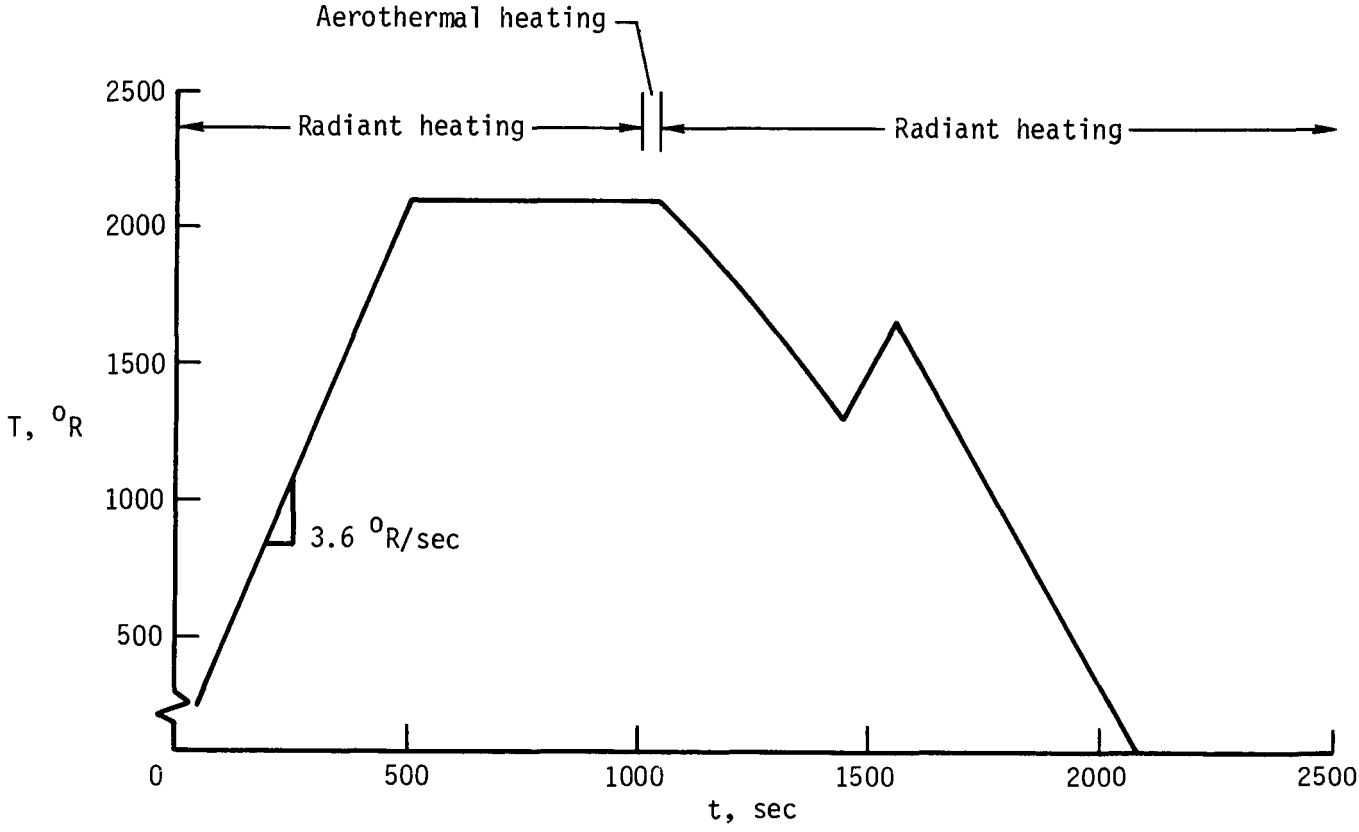

Figure 15.- Typical surface radiant-heating or radiant preheat/aerothermal-heating profile for Space Shuttle entry conditions. (Aerothermal-heating section deleted during radiant-heating tests.)

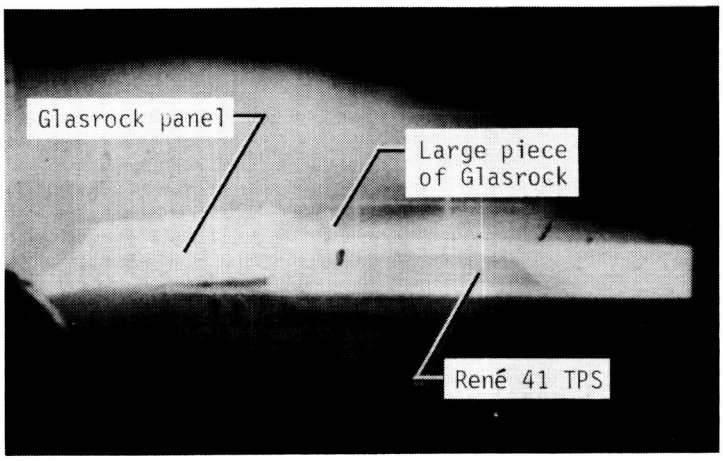

(a) Glasrock front panel lifting off surface of panel holder.

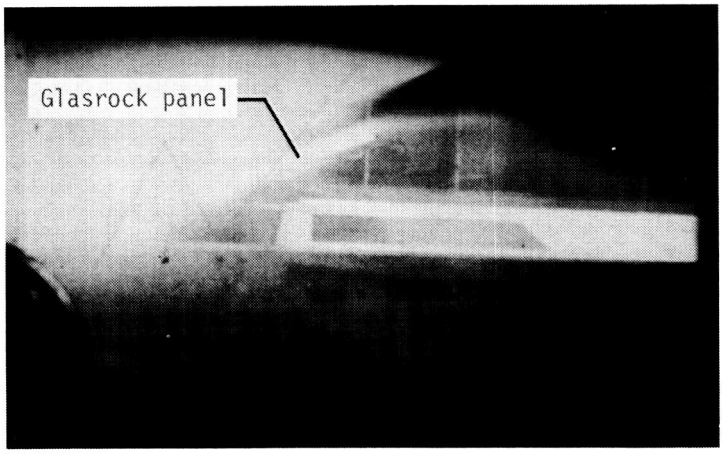

(b) Glasrock panel completely detached from panel holder.

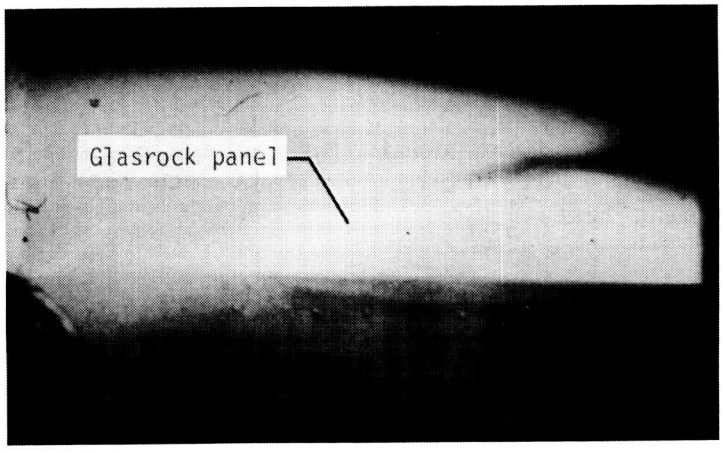

(c) Glasrock panel crushing against René 41 TPS model.

L-84-45

Figure 16.- Sequence of events leading to damage of René 41 TPS model.

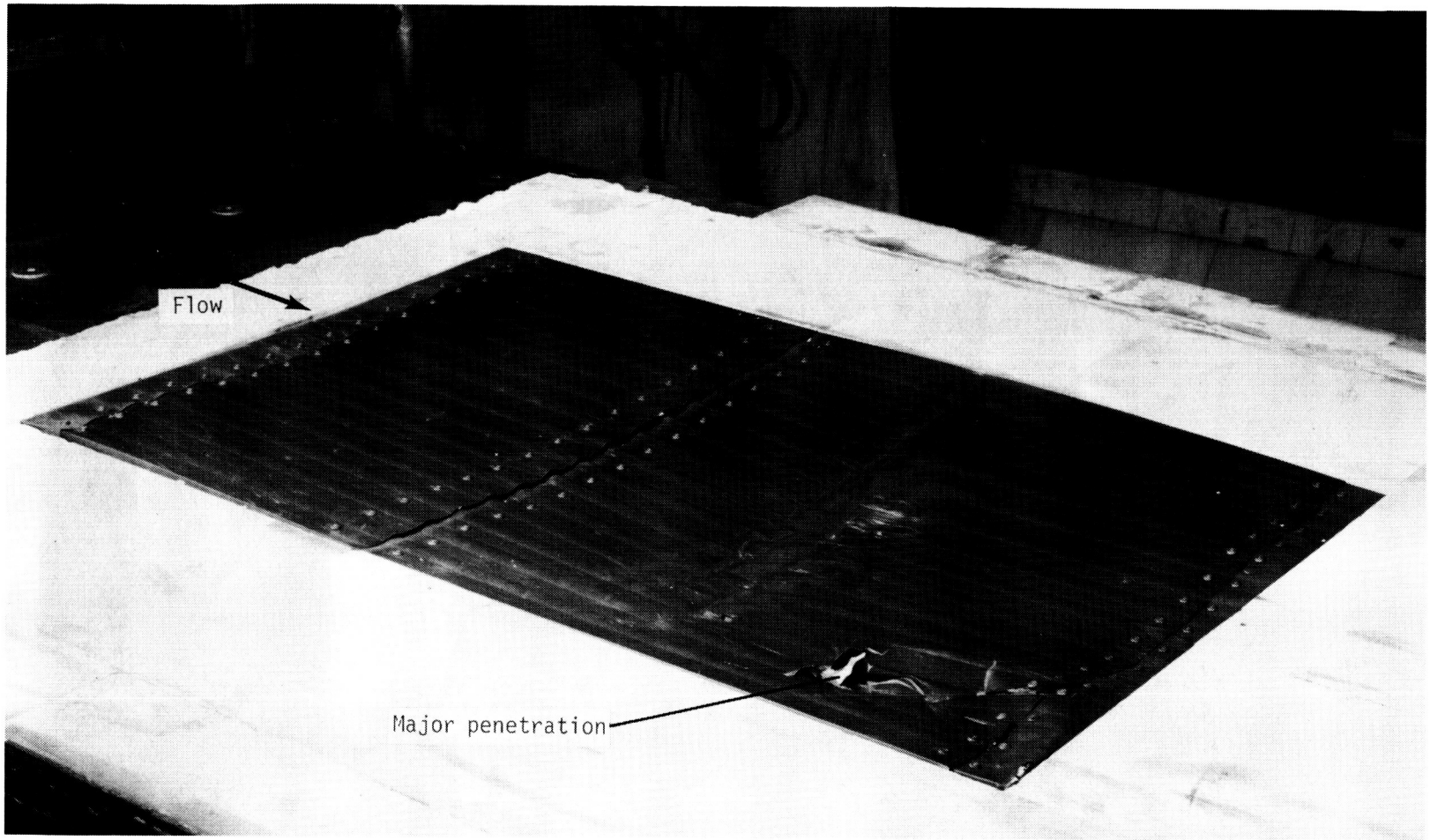

L-81-3509.1

(a) Damage after test 11.

Figure 17.- Penetration damage to René 41 TPS model because of leading-edge Glasrock detachment (flow from left).

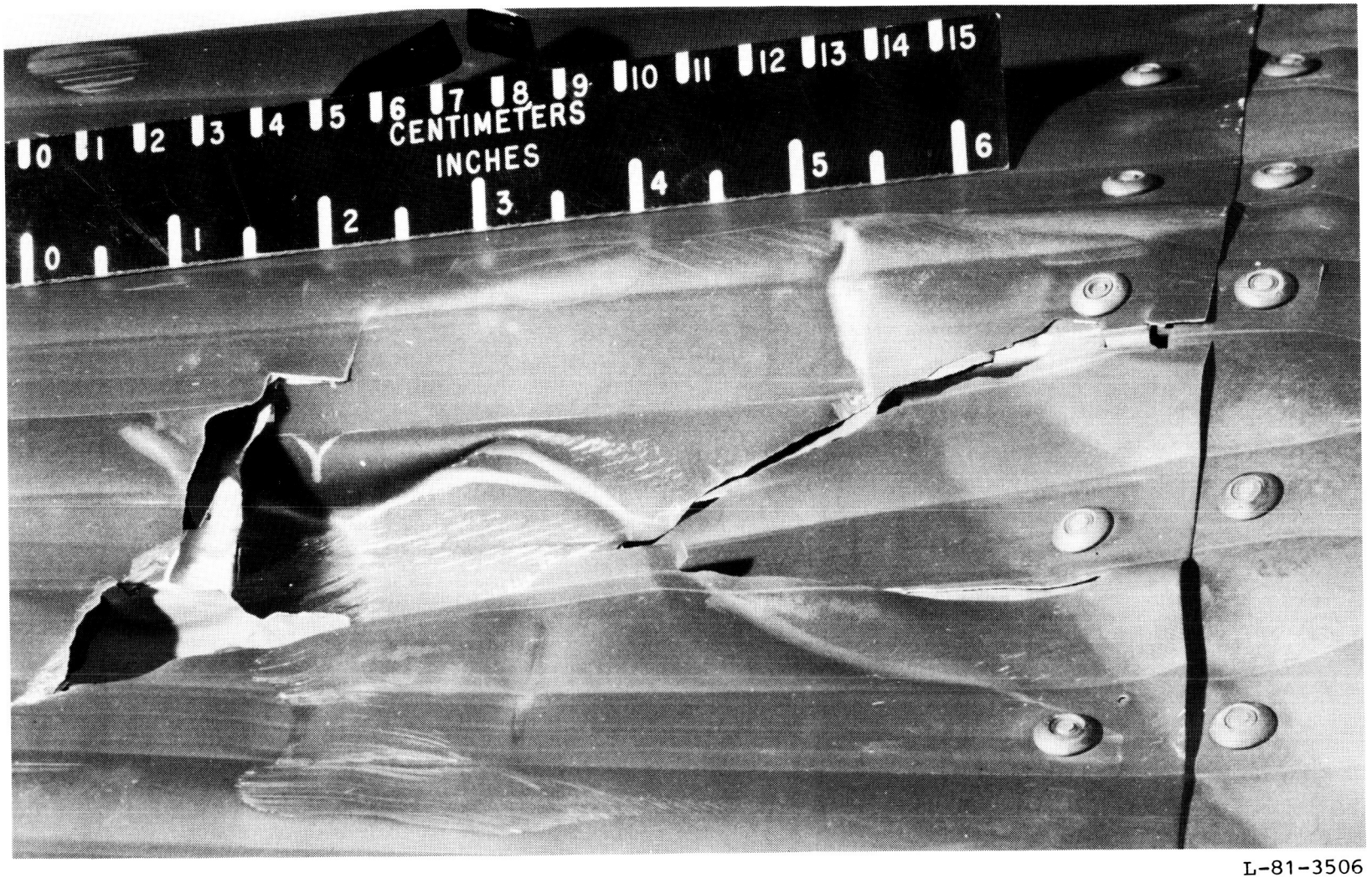

L-81-3506

(b) Major penetration.

Figure 17.- Concluded.

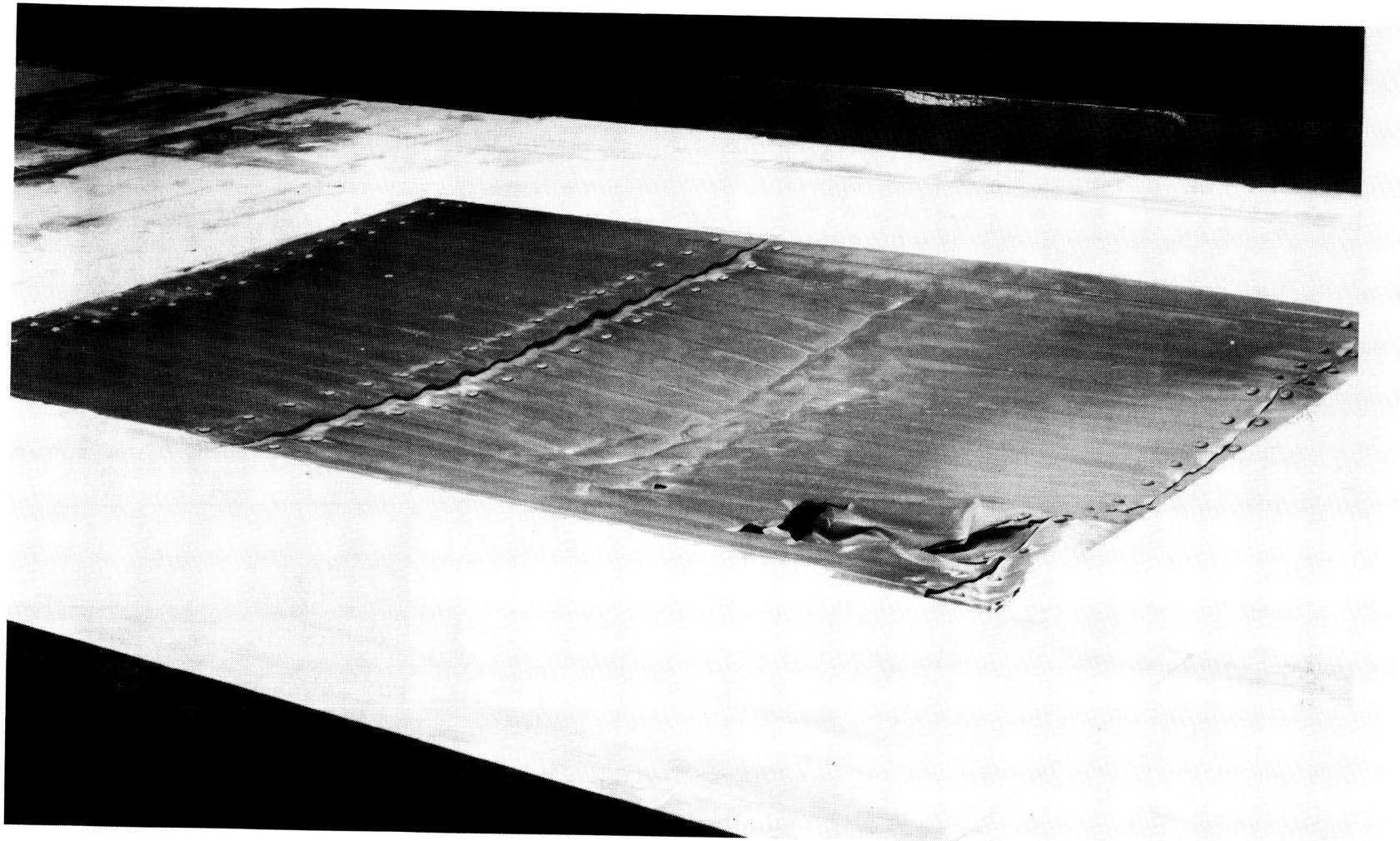

L-81-3964

(a) Overall model condition after test 13.

Figure 18.- Penetration-damaged René 41 TPS model after two radiant preheat/aerothermal exposures.

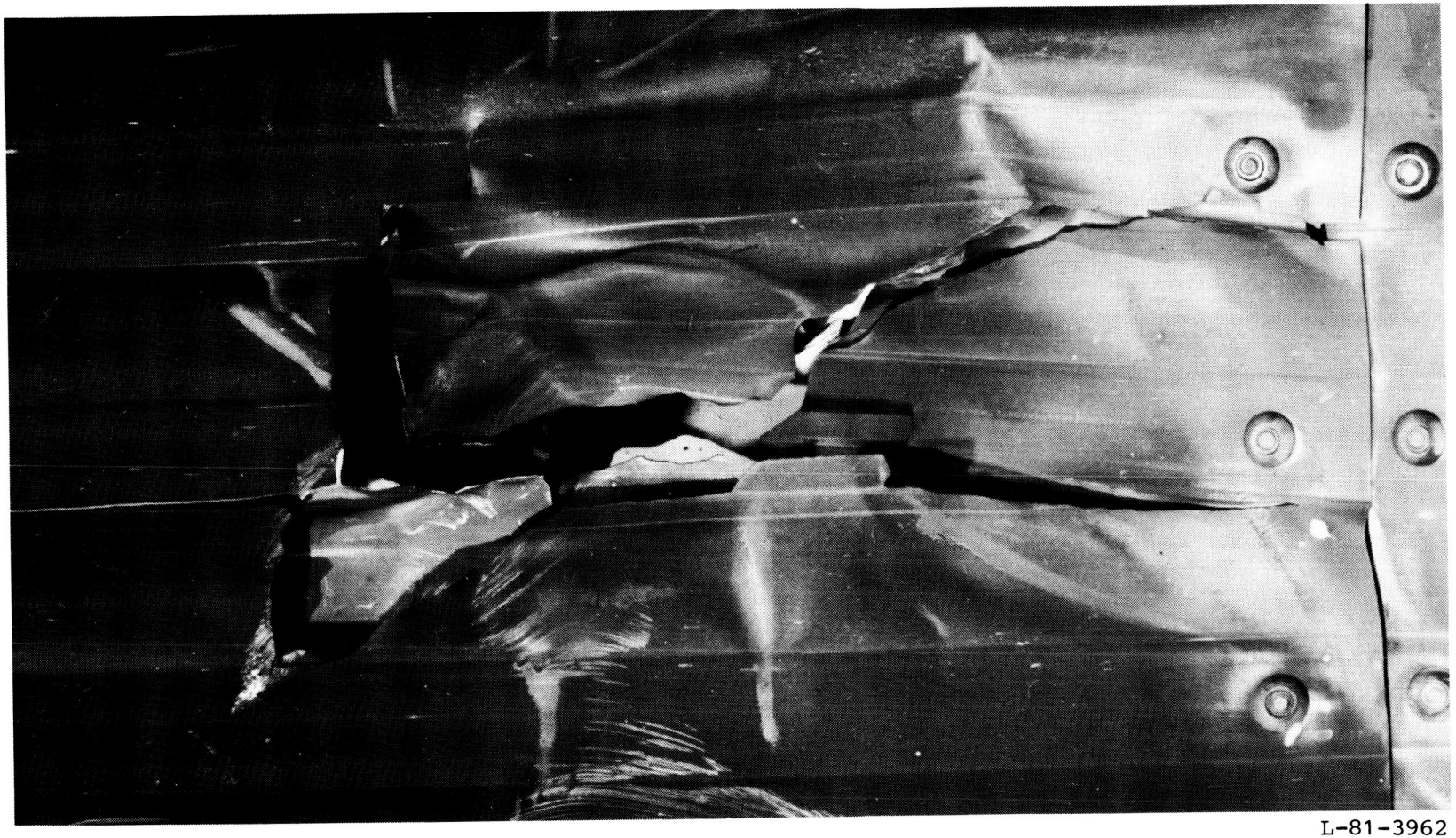

L-81-3962

(b) Major penetration condition after test 13.

Figure 18.- Concluded.

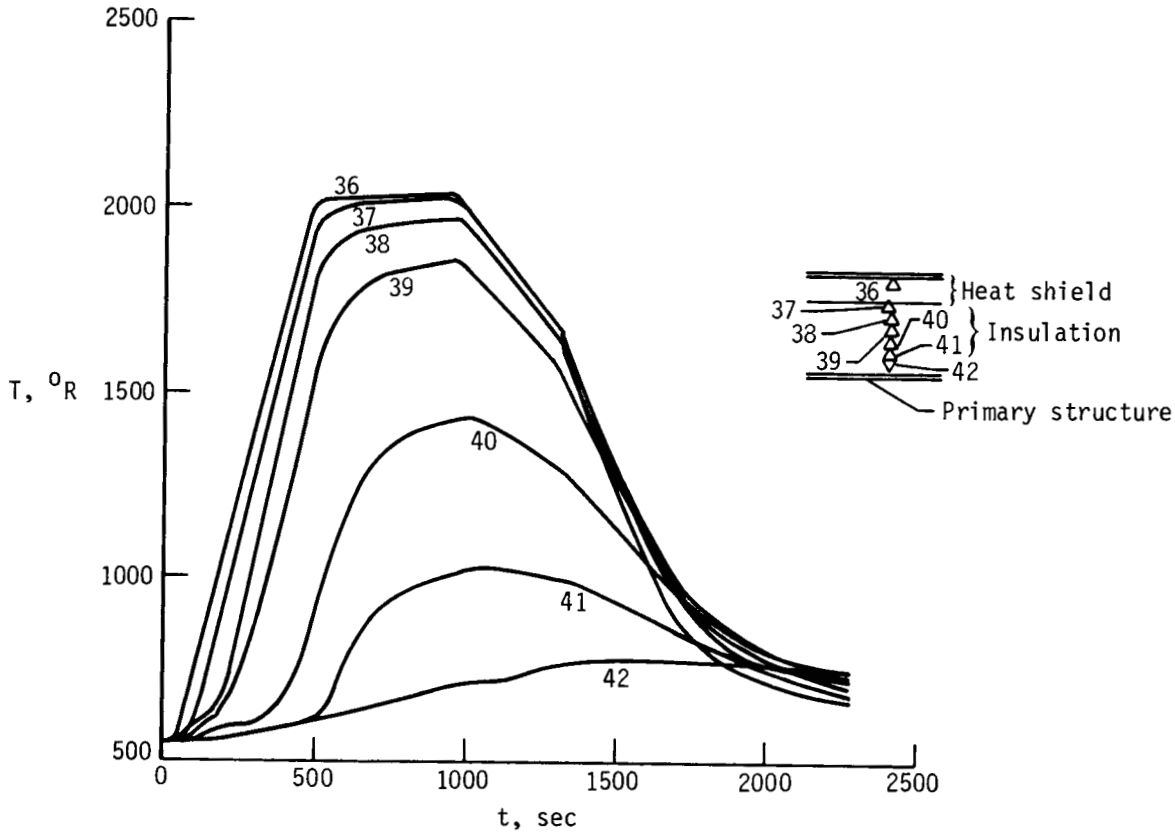

(a) Test 2 (radiant-heating test).

Figure 19.- Temperature distributions on heat shield, through the insulation, and on the primary structure.

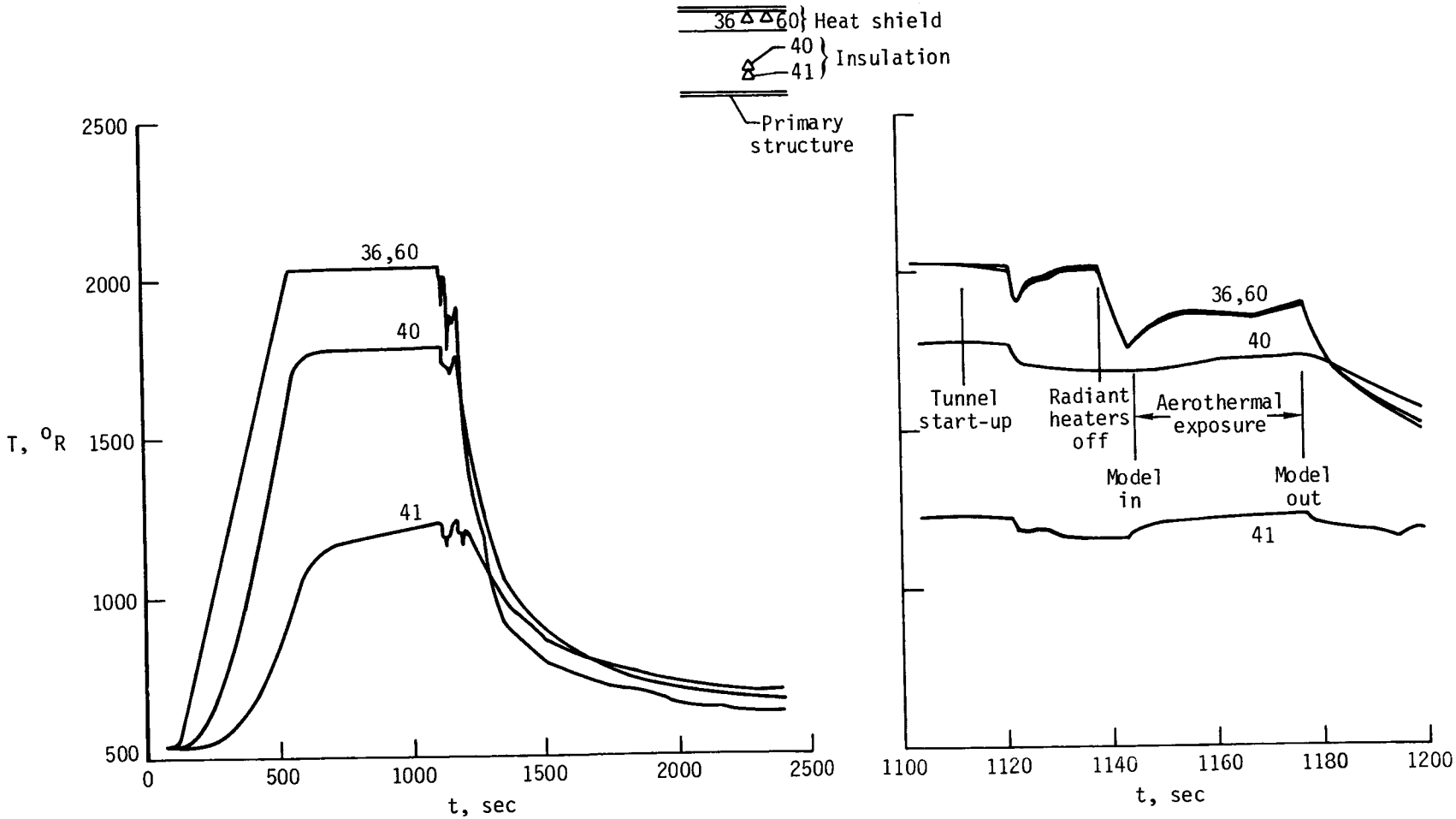

(b) Test 13 (radiant preheat/aerothermal-heating test).

Figure 19.- Concluded.

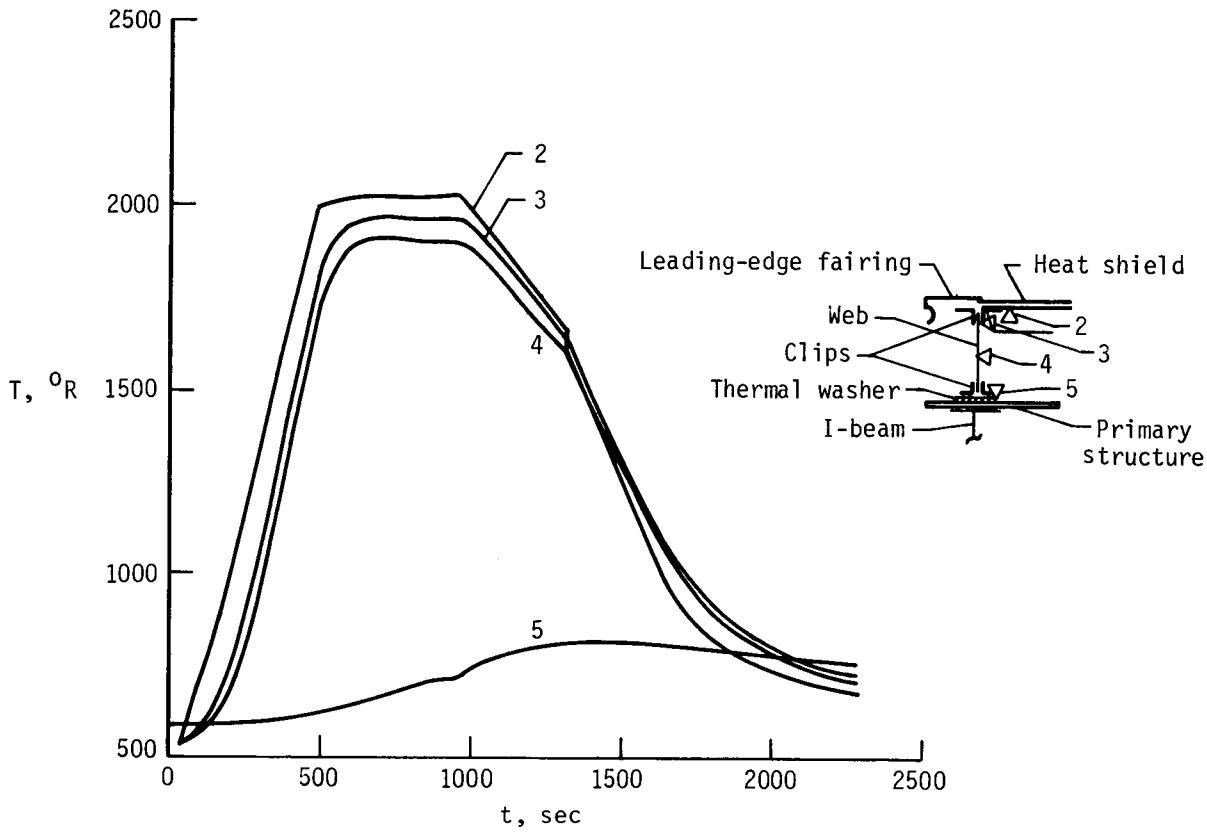

(a) Test 2 (radiant-heating test).

Figure 20.- Temperature response of heat shield, support, and primary structure.

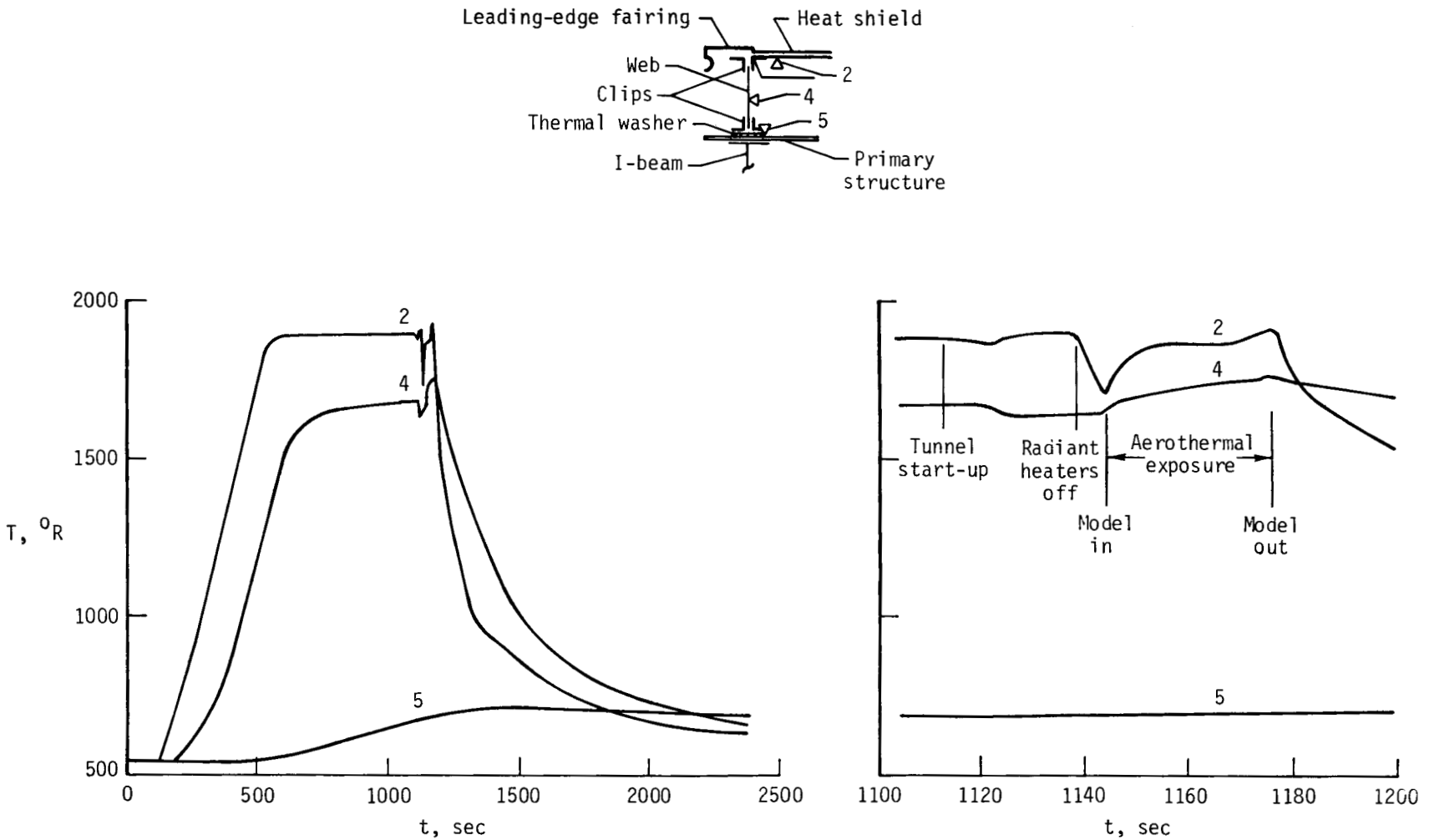

(b) Test 13 (radiant preheat/aerothermal-heating test).

Figure 20.- Concluded.

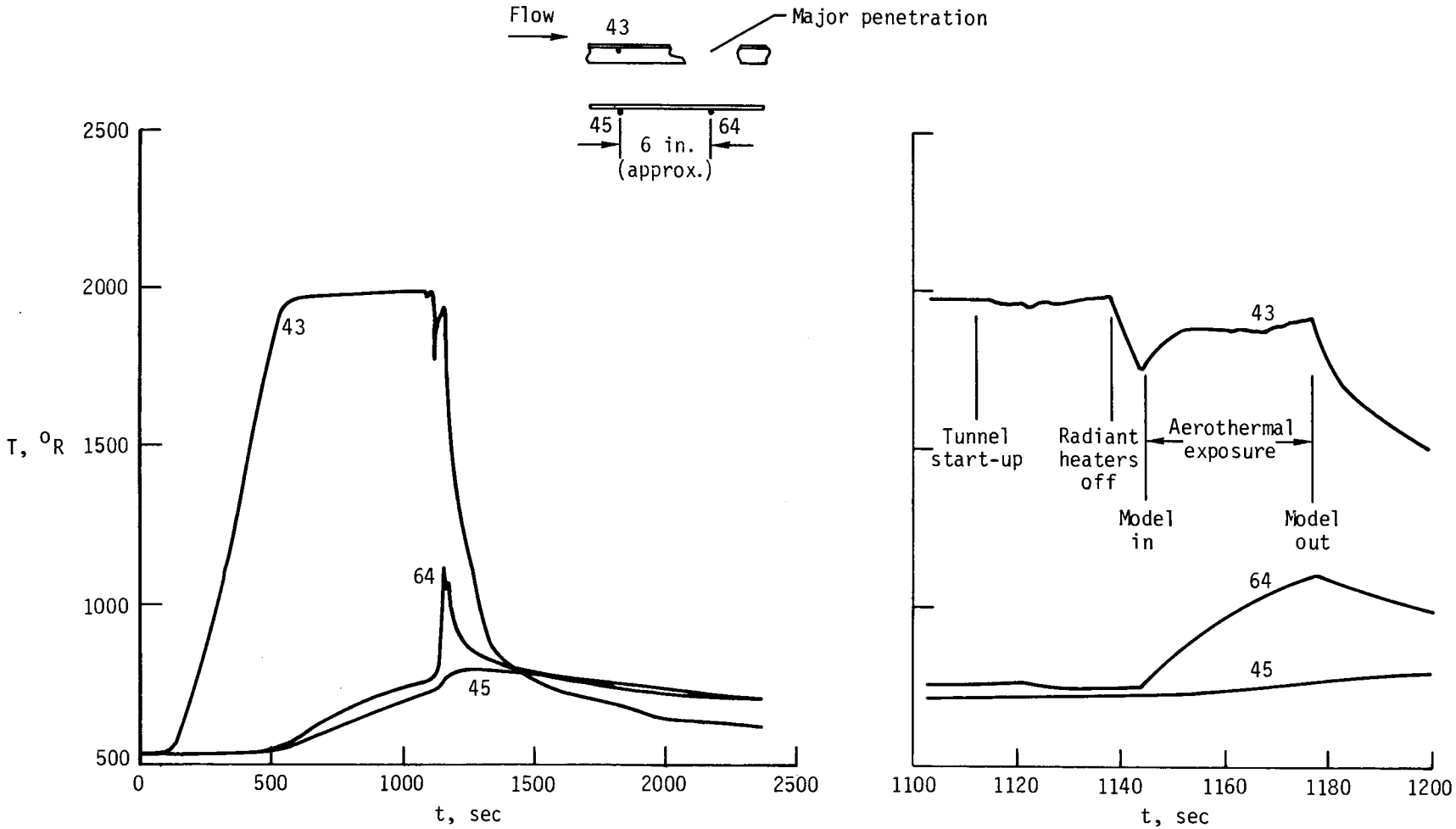

Figure 21.- Temperature response of heat shield and primary structure during radiant preheat/aerothermal-heating test in area of major penetration (test 13).

1. Report No.	2. Government Accession No.	3. Recipient's Catalog No.
NASA TM-85773		

4. Title and Subtitle	5. Report Date
AEROTHERMAL PERFORMANCE AND DAMAGE TOLERANCE OF A RENÉ 41 METALLIC STANDOFF THERMAL PROTECTION SYSTEM AT MACH 6.7	July 1984
	6. Performing Organization Code 506-53-33-04
7. Author(s) Don E. Avery	8. Performing Organization Report No. L-15772
	10. Work Unit No.
9. Performing Organization Name and Address NASA Langley Research Center Hampton, VA 23665	11. Contract or Grant No.
	13. Type of Report and Period Covered Technical Memorandum
12. Sponsoring Agency Name and Address National Aeronautics and Space Administration Washington, DC 20546	14. Sponsoring Agency Code

15. Supplementary Notes

16. Abstract

A flight-weight, metallic thermal protection system (TPS) model applicable to Earth-entry and hypersonic-cruise vehicles was subjected to multiple cycles of both radian and aerothermal heating in order to evaluate its aerothermal performance, structural integrity, and damage tolerance. The TPS was designed for a maximum operating temperature of 2060°R and featured a shingled, corrugation-stiffened corrugated-skin heat shield of René 41, a nickel-base alloy. The model was subjected to 10 radiant-heating tests and to 3 radiant preheat/aerothermal tests. Under radiant-heating conditions with a maximum surface temperature of 2050°R, the TPS performed as designed and limited the primary structure away from the support ribs to temperatures below 780°R. During the first attempt at aerothermal exposure, a failure in the panel-holder test fixture severely damaged the model. However, two radiant preheat/aerothermal tests were made with the damaged model to test its damage tolerance. During these tests, the damaged area did not enlarge; however, the rapidly increasing structural temperature measured during these tests indicates that had the damaged area been exposed to aerodynamic heating for the entire trajectory, an aluminum burn-through would have occurred.

17. Key Words (Suggested by Author(s))	18. Distribution Statement
Thermal protection system René 41 Space Shuttle Hypersonic-cruise vehicles	Unclassified - Unlimited Subject Category 18

19. Security Classif. (of this report)	20. Security Classif. (of this page)	21. No. of Pages	22. Price
Unclassified	Unclassified	39	A03

For sale by the National Technical Information Service, Springfield, Virginia 22161 NASA-Langley,